SUPPLEMENTARY INFORMATION FOR

Diversity-Oriented Combinatorial Biosynthesis of Hybrid Polyketide Scaffolds from Azaphilone and Benzenediol Lactone Biosynthons

Jing Bai[§,†,‖], Yuanyuan Lu[†,‡,‖], Ya-ming Xu[†], Wei Zhang[§], Ming Chen[§], Min Lin[§], A. A. Leslie Gunatilaka[†], Yuquan Xu[§,*], and István Molnár[†,*]

[§]Biotechnology Research Institute, The Chinese Academy of Agricultural Sciences, 12 Zhongguancun South St., Beijing 100081, P. R. China

[†]Natural Products Center, School of Natural Resources and the Environment, The University of Arizona, 250 East Valencia Rd., Tucson, Arizona 85706, United States

[‡]State Key Laboratory of Natural Medicines, School of Life Science and Technology, China Pharmaceutical University, 24 Tong Jia Xiang, Nanjing 210009, P. R. China

[‖]These authors contributed equally.

*Corresponding authors: imolnar@email.arizona.edu (I. Molnár); xuyuquan@caas.cn (Y. Xu)

Table of Contents

1. SI Materials and Methods

1.1. Molecular cloning

The construction of the YEpCcRadS1, YEpCcRadS2, YEpAtCurS1, YEpAtCurS2, YEpLtLasS1, YEpLtLasS2, YEpAzResS1 and YEpAzResS2 expression vectors has been described elsewhere.[1-4] The Udwary-Merski algorithm was used to predict domain boundaries in iPKSs.[5] The primers used in this study are listed in Table S1.

The plasmid YEpAfoG was constructed to express the *A. nidulans afoG* gene encoding the AfoG hrPKS for asperfuranone biosynthesis. The intronless AfoG hrPKS gene was reconstituted by Gibson assembly (New England Biolabs) in pJET1.2 (Thermo Scientific), using the Phusion polymerase (Thermo Scientific) to amplify gene segments on *A. nidulans* FGSC A4 genomic DNA as the template. The *afoG* open reading frame (ORF) was reconstructed from five parts: a 204-bp fragment (amplified with primers AfoG_1_F and AfoG_1_R), a 104-bp fragment (amplified with primers AfoG_2_F and AfoG_2_R), a 79-bp fragment (amplified with primers AfoG_3_F and AfoG_3_R), a 1,963-bp fragment (amplified with primers AfoG_4_1_F and AfoG_4_1_R), and a 5,569-bp fragment (amplified with primers AfoG_4_2_F and AfoG_4_2_R). After sequence verification, the intronless *afoG* hrPKS gene fragment was ligated as an *Nde*I - *Pme*I fragment into the corresponding sites of YEpADH2p-FLAG-TRP[4] to yield YEpAfoG.

The plasmid YEpAfoE was constructed to express the *A. nidulans afoE* gene encoding the AfoE nrPKS for asperfuranone biosynthesis. The intronless *afoE* nrPKS gene was reconstituted by Gibson assembly

(New England Biolabs) in pJET1.2 (Thermo Scientific), using the Phusion polymerase (Thermo Scientific) to amplify gene segments on *A. nidulans* FGSC A4 genomic DNA as the template. The *afoE* ORF was reconstructed from three parts: a 4,701-bp fragment (amplified with primers AfoE_1_F and AfoE_1_R), a 3,294-bp fragment (amplified with primers AfoE_2_F and AfoE_2_R), and a 360-bp fragment (amplified with primers amplified with primers AfoE_3_F and AfoE_3_R). After sequence verification, the intronless *afoE* nrPKS was ligated as an *Nde*I - *Pme*I fragment into the corresponding sites of YEpADH2p-FLAG-URA[4] to yield YEpAfoE.

The plasmid YEpAfoC was constructed to express the *A. nidulans afoC* gene encoding the AfoC putative esterase/lipase for asperfuranone biosynthesis. The ADH2 promoter-polylinker-ADH2 terminator cassette of YEpADH2p-FLAG-URA[4] was moved into pRS425[6] as a *Not*I - *Xho*I fragment to generate YEpADH2p-FLAG-Leu. The 911-bp intronless *afoC* gene was amplified with primers AfoC_F (NdeI) and AfoC_R (*Pme*I) was cloned into pJET1.2 and sequence verified. The *afoC* gene was ligated as an *Nde*I - *Pme*I fragment into the corresponding sites of YEpADH2p-FLAG-Leu to yield YEpAfoC.

The plasmid YEpAzResS2-SAT_{AfoE} is based on YEpADH2p-FLAG-URA,[4] and carries the intronless *azresS2* gene in which the gene segment encoding $SAT_{AzResS2}$ was replaced by the one encoding SAT_{AfoE}. Using YEpAfoE as the template, a 1,265-bp fragment encoding M^{1} to P^{413} of AfoE was amplified with primers AfoESAT_ResS2_F (*Nde*I) and AfoESAT_ResS2_R. Using YEpAzResS2 as a template, a 597-bp fragment encoding G^{392} to S^{590} of AzResS2 was amplified with primers ResS2_AfoESAT_Dn_F and ResS2_AfoESAT_Dn_R (*Sex*A1). These two PCR fragments were then fused using primers AfoESAT_ResS2_F (*Nde*I) and ResS2_AfoESAT_Dn_R (*Sex*A1), and cloned into pJET1.2. After sequence

verification, the *Nde*I - *Sex*A1 fragment was inserted into the equivalent cloning sites of YEpAzResS2 to yield plasmid YEpAzResS2-SAT_{AfoE}.

The plasmid YEpLtLasS2-SAT_{AfoE} is based on YEpADH2p-FLAG-URA,[4] and carries the intronless LtLasS2 gene in which the gene segment encoding $SAT_{LtLasS2}$ was replaced by the one encoding SAT_{AfoE}. Using YEpAfoE as the template, a 1,266-bp fragment encoding M^1 to P^{413} of AfoE was amplified with primers AfoESAT_ResS2_F (*Nde*I) and AfoESAT_LasS2_R. Using YEpLtLasS2 as a template, a 668-bp fragment encoding T^{358} to G^{579} of LtLasS2 was amplified with primers LasS2_AfoESAT_Dn_F and LasS2_AfoESAT_Dn_R (*Blp*I). These two PCR fragments were then fused using primers AfoESAT_ResS2_F (*Nde*I) and LasS2_AfoESAT_Dn_R (*Blp*I), and cloned into pJET1.2. After sequence verification, the *Nde*I - *Blp*I fragment was inserted into the equivalent cloning sites of YEpLtLasS2 to yield plasmid YEpLtLasS2-SAT_{AfoE}.

The plasmid YEpAtCurS2-SAT_{AfoE} is based on YEpADH2p-FLAG-URA,[4] and carries the intronless AtCurS2 gene in which the gene segment encoding $SAT_{AtCurS2}$ was replaced by the one encoding SAT_{AfoE}. Using YEpAfoE as the template, a 1,928-bp fragment encoding M^1 - P^{427} of AfoE was amplified with primers AfoESAT_CurS2_F (*Not*I) and AfoESAT_CurS2_R. Using YEpLtLasS2 as a template, a 1,005-bp fragment encoding K^{359} - D^{686} of AtCurS2 was amplified with primers CurS2_AfoESAT_Dn_F and CurS2_AfoESAT_Dn_R (*Bsu*36I). These two PCR fragments were then fused using primers AfoESAT_CurS2_F (*Not*I) and CurS2_AfoESAT_Dn_R (*Bsu*36I), and cloned into pJET1.2. After sequence verification, the *Not*I-*Bsu*36I fragment was inserted into the equivalent cloning sites of YEpAtCurS2 to yield plasmid YEpAtCurS2-SAT_{AfoE}.

The plasmid YEpCcRadS2-SAT$_{AfoE}$ is based on YEpADH2p-FLAG-URA,[4] and carries the intronless CcRadS2 gene in which the gene segment encoding SAT$_{CcRadS2}$ was replaced by the one encoding SAT$_{AfoE}$. Using YEpAfoE as the template, a 1,265-bp fragment encoding M^{1} - P^{413} of AfoE was amplified with primers AfoESAT_RadS2_F (*Nde*I) and AfoESAT_RadS2_R. Using YEpCcRadS2 as a template, a 1,554-bp fragment encoding Q^{364} - L^{880} of CcRadS2 was amplified with primers RadS2_AfoESAT_Dn_F and RadS2_AfoESAT_Dn_R (*Age*I). These two PCR fragments were then fused using primers AfoESAT_RadS2_F (*Nde*I) and RadS2_AfoESAT_Dn_R (*Age*I), and cloned into pJET1.2. After sequence verification, the *Nde*I - *Age*I fragment was inserted into the equivalent cloning sites of YEpCcRadS2 to yield plasmid YEpCcRadS2-SAT$_{AfoE}$.

The plasmid YEpAfoE-SAT$_{CcRadS2}$ is based on YEpADH2p-FLAG-URA,[4] and carries the intron-less AfoE gene in which the gene segment encoding SAT$_{AfoE}$ was replaced by the one encoding SAT$_{CcRadS2}$. Using YEpCcRadS2 as the template, a 1,151-bp fragment encoding M^{1} - V^{367} of CcRadS2 was amplified with primers RadS2SAT_AfoE_F (*Nde*I) and RadS2SAT_AfoE_R. Using YEpAfoE as a template, a 887-bp fragment encoding L^{415} - N^{708} of AfoE was amplified with primers AfoE_RadS2SAT_Dn_F and AfoE_RadS2SAT_Dn_R (*Sex*A1). These two PCR fragments were then fused using primers RadS2SAT_AfoE_F (*Nde*I) and AfoE_RadS2SAT_Dn_R (*Sex*AI) and cloned into pJET1.2. After sequence verification, the *Nde*I - *Sex*A1 fragment was inserted into the equivalent cloning sites of YEpAfoE to yield plasmid YEpAfoE-SAT$_{CcRadS2}$.

The plasmid YEpAfoE-SAT$_{LtLasS2}$ is based on YEpADH2p-FLAG-URA,[4] and carries the intronless AfoE gene in which the gene segment encoding SAT$_{AfoE}$ was replaced by the one encoding SAT$_{LtLasS2}$. Using

YEpLtLasS2 as the template, a 1,729-bp fragment encoding M^{1} - Q^{357} of LtLasS2 was amplified with primers LasS2SAT_AfoE_F (*Not*I) and LasS2SAT_AfoE_R. Using YEpAfoE as a template, a 887-bp fragment encoding V^{414} - N^{708} of AfoE was amplified with primers AfoE_LasS2SAT_Dn_F and AfoE_LasS2SAT_Dn_R (*Sex*AI). These two PCR fragments were then fused using primers LasS2SAT_AfoE_F (*Not*I) and AfoE_LasS2SAT_Dn_R (*Sex*AI), and cloned into pJET1.2. After sequence verification, the *Not*I - *Sex*A1 fragment was inserted into the equivalent cloning sites of YEpAfoE to yield plasmid YEpAfoE-$SAT_{LtLasS2}$.

The plasmid YEpAfoE-$SAT_{AzResS2}$ is based on YEpADH2p-FLAG-URA,[4] and carries the intronless AfoE gene in which the gene segment encoding SAT_{AfoE} was replaced by the one encoding $SAT_{AzResS2}$. Using YEpAzResS2 as the template, a 1,817-bp fragment encoding M^{1} - D^{391} of AzResS2 was amplified with primers ResS2SAT_AfoE_F (*Not*I) and ResS2SAT_AfoE_R. Using YEpAfoE as a template, a 2,117-bp fragment encoding V^{428} - N^{1126} of AfoE was amplified with primers AfoE_ResS2SAT_Dn_F and AfoE_ResS2SAT_Dn_R (*Spe*I). These two PCR fragments were then fused using primers ResS2SAT_AfoE_F (*Not*I) and AfoE_ResS2SAT_Dn_R (*Spe*I), and cloned into pJET1.2. After sequence verification, the *Not*I - *Spe*I fragment was inserted into the equivalent cloning sites of YEpAfoE to yield plasmid YEpAfoE-$SAT_{AzResS2}$.

The plasmid YEpAfoE-$SAT_{AtCurS2}$ is based on YEpADH2p-FLAG-URA,[4] and carries the intronless AfoE gene in which the gene segment encoding SAT_{AfoE} was replaced by the one encoding $SAT_{AtCurS2}$. Using YEpAtCurS2 as the template, a 1,718-bp fragment encoding M^{1} - A^{358} of AtCurS2 was amplified with primers CurS2SAT_AfoE_F (*Not*I) and CurS2SAT_AfoE_R. Using YEpAfoE as a template, a 2,117-bp

fragment encoding V^{428} - N^{1126} of AfoE was amplified with primers AfoE_CurS2SAT_Dn_F and AfoE_CurS2SAT_Dn_R (*Spe*I). These two PCR fragments were then fused using primers CurS2SAT_AfoE_F (*Not*I) and AfoE_CurS2SAT_Dn_R (*Spe*I), and cloned into pJET1.2. After sequence verification, the *Not*I - *Spe*I fragment was inserted into the equivalent cloning sites of YEpAfoE to yield plasmid YEpAfoE-$SAT_{AtCurS2}$.

1.2. Chemical characterization of polyketide products

1.2.1. General methods

Analytical thin-layer chromatography was carried out on silica gel 60 F254 aluminum-backed TLC plates (Merck). Compounds were visualized with short-wavelength UV and by spraying with anisaldehyde-sulfuric acid spray reagent and heating. ODS-C18 (YMC, 40-63 µm) and silica gel (Merck, 40-70 µm) were used for chromatography. Metabolites were routinely analyzed and isolated with a reversed-phase C18 column (Kromasil 5 µm, 4.6 mm × 250 mm) on an Agilent 1050 HPLC instrument. ^{1}H NMR, ^{13}C NMR, 1D-NOESY, and 2D NMR (^{1}H-^{1}H COSY, HSQC, and HMBC) spectra were obtained on a Bruker Avance III 400 spectrometer at 400 MHz for ^{1}H NMR and 100 MHz for ^{13}C NMR. Chemical shift values (δ) are given in parts per million (ppm), and the coupling constants (*J* values) are in Hz. Chemical shifts were referenced to the residual solvent peaks of CD_3OD, CD_3COCD_3 and $CDCl_3$ respectively. Optical rotations were measured on a *Jasco* DIP-370 Digital polarimeter using a 10 cm microcell. Accurate mass measurements and liquid chromatography-mass spectrometry (LC-MS) were carried out on a Mariner

ESI-TOF spectrometer coupled with an Agilent 1200 HPLC instrument. All yields mentioned in the text refer to the yields of isolated compounds. Unless otherwise stated, chemicals and solvents were of reagent grade and used as obtained from commercial sources.

1.2.2. Small scale fermentation and product analysis

Typically, a yeast strain was cultured in 50 mL of SC medium (0.67% yeast nitrogen base, 2% glucose, 0.72 g/L Trp/Ura DO supplement [Clontech]) at 30 °C with shaking at 220 rpm. When the OD_{600} reached 0.6, an equal volume of YP medium (1% yeast extract, 2% peptone) was added to the culture, and the fermentation was continued under the same conditions for an additional 2 days. The culture was then adjusted to pH 5.0, and extracted with ethyl acetate three times. The extract was evaporated to dryness and analyzed by reversed phase HPLC (Kromasil C18 column, 5 µm, 4.6 mm × 250 mm; eluted with 5% acetonitrile in water for 5 min followed by a linear gradient of 5-95% of acetonitrile-water over 10 min, and 95% acetonitrile-water for 10 min at a flow rate of 0.8 mL/min; detection at 214, 280, and 300 nm).

1.2.3. Large scale fermentation and compounds isolation

For a typical large scale culture, multiple 250mL flasks, each containing 50 mL of SC medium, were inoculated with a yeast strain and cultured at 30 °C with shaking at 220 rpm. After the OD_{600} reached 1.0, 50 mL of YP medium was added to each flask. The culture was harvested 3 days later by centrifugation at 6,000 rpm for 10 min to remove yeast cells. The supernatant was concentrated to 200 mL. The solution was adjusted to pH 5.0, and extracted with 600 mL of ethyl acetate three times.

1.2.4. Isolation of compounds 6 and 8-17

The dried EtOAc extract (1.3 g) from a 2 L fermentation broth of *Saccharomyces cerevisiae* BJ5464-NpgA[7,8] carrying YEpAfoG and YEpAfoE was subjected to ODS column chromatography (YMC, 40 µm, 20 × 60 mm) and eluted with MeOH and H_2O (Fraction A, H_2O, 100 mL; Fraction B, 1/1, 50 mL; Fraction C, 3/2, 200 mL; Fraction D, 4/1, 250 mL; Fraction E, MeOH, 200 mL; v/v). Pre-asperfuranone (**6**, 10.2 mg) was obtained from Fraction D.

The dried EtOAc extract (1.1 g) from 3.5 L fermentation broth of *S. cerevisiae* BJ5464-NpgA[7,8] carrying YEpCcRadS1 and YEpAfoE-$SAT_{CcRads2}$ was subjected to ODS column chromatography and eluted with MeOH and H_2O (Fraction A, H_2O; Fraction B, 1/1; Fraction C, 3/2; Fraction D, MeOH; v/v, each 200 mL). Compound **8** (1.1 mg, retention time: 13 min) was isolated from Fraction C by reversed phase HPLC (MeCN/H_2O/TFA = 25/75/0.1, v/v).

The dried EtOAc extract (1.1 g) from 3.8 L fermentation broth of *S. cerevisiae* BJ5464-NpgA[7,8] carrying YEpLtLasS1 and YEpAfoE-$SAT_{LtLasS2}$ was subjected to ODS column chromatography (YMC, 40 µm, 20 × 60 mm) and eluted with MeOH and H_2O (Fraction A, H_2O; Fraction B, 2/3; Fraction C, 1/1; Fraction D, 3/2; Fraction E, MeOH; v/v, each 150 mL). Fraction C was further purified by silica gel chromatography (Merck, 40 µm, 10 × 50 mm) and eluted with hexanes-EtOAc mixtures of increasing polarity (fraction 1, Hexanes; fraction 2, 3/1; fraction 3, 3/1; fraction 4, EtOAc; v/v, each 60 mL). Compound **9** (9.0 mg) was obtained from Fraction 3.

The dried EtOAc extract (1.2 g) from 4.0 L fermentation broth of *S. cerevisiae* BJ5464-NpgA[7,8] carrying YEpADH2p-FLAG-TRP and YEpAfoE-$SAT_{LtLasS2}$ was subjected to ODS column chromatography (YMC, 40 µm,

20 × 60 mm) and eluted with MeOH/H_2O (1/1, 3/2, 7/3, and 9/1, v/v, each 150 mL) to afford Fraction A-D. Compounds **10** (2.1 mg, t_R = 18.1 min) and **11** (0.2 mg, t_R = 16.1 min) were obtained from Fraction C by reversed phase HPLC (MeCN/H_2O = 85/15, v/v).

The dried EtOAc extract (1.6 g) from a 1.7 L culture broth of *S. cerevisiae* BJ5464-NpgA[7,8] carrying YEpAfoG and YEpAtCurS2-SAT_{AfoE} was subjected to ODS column chromatography (YMC, 40 μm, 20 × 60 mm) and eluted with MeOH and H_2O (Fraction A, H_2O, 100 mL; Fraction B, MeOH/H_2O = 1/1, v/v, 50 mL; Fraction C, MeOH/H_2O = 3/2, v/v, 200 mL; Fraction D, MeOH/H_2O = 4/1, v/v, 250 mL; Fraction E, MeOH, 200 mL). Compound **12** (1.2 mg, t_R = 15 min) was isolated from Fraction C by reversed phase HPLC (MeCN/H_2O = 1/1, v/v). Compound **13** (0.5 mg, t_R = 20 min) was obtained from Fraction E by reversed phase HPLC (MeCN/H_2O = 4/1, v/v).

The EtOAc extract (1.2 g) of a 4 L fermentation broth of *S. cerevisiae* BJ5464-NpgA[7,8] carrying YEpAfoG and YEpLtLasS2-SAT_{AfoE} was subjected to ODS column chromatography (YMC, 40 μm, 20 × 60 mm) and eluted with MeOH/H_2O (2/3, 1/1, 3/2, 7/3, and 9/1, v/v, each 150 mL) to afford Fractions A-E. Fractions D and E, which contained the same two compounds, were further separated by silica gel chromatography (Merck, 40 μm, 10 × 50 mm, hexanes/EtOAc (Hexanes, 10/1, 8/1, 6/1, and EtOAc, v/v, each 60 mL) affording Fractions 1-5. Fraction 4 and Fraction 3 were further purified by reversed phase HPLC to give **14** (0.7 mg, t_R = 15 min, MeOH/H_2O = 4/1, v/v) and **15** (0.8 mg, t_R = 70 min, MeCN/H_2O = 56/44, v/v), respectively. Compound **14** (0.5 mg) was also obtained from the EtOAc extract of a 2 L fermentation broth of *S. cerevisiae* BJ5464-NpgA[7,8] carrying YEpAfoG and YEpAzResS2-SAT_{AfoE} using an identical isolation process.

The dried EtOAc extract (3.3 g) from a 10 L fermentation broth of *S. cerevisiae* BJ5464-NpgA[7,8] carrying YEpAfoG and YEpAtCurS2-SAT_{AfoE} was subjected to ODS column chromatography (YMC, 40 μm, 20 × 60 mm) and eluted with MeOH and H_2O (Fraction A, H_2O, 100 mL; Fraction B, 1/1, 50 mL; Fraction C, 3/2, 200 mL; Fraction D, 4/1, 250 mL; Fraction E, MeOH, 200 mL; v/v). Compounds **12** (2.2 mg, t_R = 15 min), **16** and **17** (1.3 mg, t_R = 21 min) were isolated from Fraction C by reversed phase HPLC (MeCN: H_2O = 1:1, 0.1% TFA, v/v). Compound **13** (0.5 mg, t_R = 20 min) was obtained from Fraction E by reversed phase HPLC (MeCN: H_2O = 4:1, v/v) .

1.2.5. Data for compounds 6 and 8-17

Pre-asperfuranone **6**: ^{1}H NMR (400 MHz, CD_3COCD_3) δ_H: 12.79 (1H, s), 9.91 (1H, s), 7.36 (1H, d, *J* = 16.0 Hz), 6.47 (1H, s), 6.27 (1H, d, *J* = 16.0 Hz), 5.85 (1H, d, *J* = 9.6 Hz), 4.26 (1H, s), 2.53 (1H, m), 2.03 (3H, s), 1.82 (3H, brs), 1.42 (1H, m), 1.32 (1H, m), 0.86 (3H, t, *J* = 7.6 Hz). ^{13}C NMR (100 MHz, CD_3COCD_3) δ_c: 197.0, 195.1, 164.6, 163.5, 150.6, 149.3, 139.9, 133.1, 124.4, 113.7, 111.5, 110.6, 44.2, 35.7, 30.7, 20.4, 12.6, 12.3, 7.38. These data were in agreement with the published data for **6**.[9]

Compound **8**: Colorless oil; $[\alpha]_D^{25}$= + 6° (*c* = 0.3, MeOH); UV (MeOH) λ_{max} (log ε): 209 (3.94); ^{1}H NMR (400 MHz, $CDCl_3$) and ^{13}C NMR (100 MHz, $CDCl_3$): see SI Table S2; HR ESI-MS (*m/z*): 185.1173 $[M+H]^+$ (calcd. for $C_{10}H_{17}O_3$ 185.1172).

Compound **9**: Colorless oil; $[\alpha]_D^{25}$= - 6° (*c* = 0.9, $CHCl_3$); ^{1}H NMR (400 MHz, $CDCl_3$) δ_H: 3.77 (1H, tq, *J* = 6.2 Hz), 2.31 (2H, t, *J* = 7.6 Hz), 1.59 (2H, m), 1.30-1.50 (10H, m), 1.18 (3H, d, *J* = 6.2 Hz); ^{13}C NMR (100 MHz, $CDCl_3$) δ_c: 179.3, 68.2, 39.2, 34.0, 29.3, 29.1, 28.9, 25.6, 24.6, 23.4; HR ESI-MS (*m/z*): 211.1304 $[M+Na]^+$ (calcd. for $C_{10}H_{20}O_3Na$ 211.1304). The NMR data were in agreement with published data for **9**.[10]

Compound **10**: White amorphous powder; UV (MeOH) λ_{max} (log ε): 217 (3.86), 295 (3.73); ^{1}H NMR (400 MHz, $CDCl_3$) δ_H: 12.68 (1H, s), 9.87 (1H, s), 6.21 (1H, s), 3.89 (2H, s), 2.52 (2H, t, *J* = 7.6 Hz), 2.10 (1H, s), 1.25-1.59 (14H, m), 0.88 (3H, s); ^{13}C NMR (100 MHz, $CDCl_3$) δ_C: 207.1, 192.8, 164.3, 160.8, 137.2, 113.1, 110.6,110.4, 45.9, 42.5, 31.8, 29.4, 29.3, 29.2, 29.1, 23.7, 22.7, 14.1, 6.95; HR ESI-MS (*m/z*): 321.2061 $[M+H]^+$ (calcd for $C_{19}H_{29}O_4$ 321.2060). The NMR spectroscopic data were in agreement with the published data for **10**.[11]

Compound **11**: HR ESI-MS: m/z 293.1756 $[M+H]^+$ (calcd for $C_{17}H_{25}O_4$ 293.1748).

Compound **12**: Colorless oil; $[\alpha]_D^{25}$= + 35° (*c* = 0.19, MeOH); UV (MeOH) λ_{max} (log ε): 261 (4.35); ^{1}H NMR (400 MHz, $CDCl_3$) δ_H: 7.29 (1H, d, *J* =15.6 Hz), 5.75 (1H, d, *J* = 15.6 Hz), 5.64 (1H, d, *J* = 6.0 Hz), 2.42 (1H, m), 1.75 (3H, d, *J* = 1.2 Hz)], 1.39 (1H, m), 1.29 (1H, m), 0.96 (3H, d, *J* = 6.4 Hz), and 0.82 (3H, t, *J* = 7.6 Hz); ^{13}C NMR (100 MHz, $CDCl_3$) δ_C: 172.1, 152.3, 150.0, 131.6, 114.5, 35.0, 29.9, 20.1, 12.4, and 11.9; HR ESI-MS (*m/z*): 169.1221 $[M+H]^+$ (calcd for $C_{10}H_{17}O_2$ 169.1223). The NMR data were in agreement with the published data for **12**.[12]

Compound **13**: Colorless oil; $[\alpha]_D^{25}$= + 62° (*c* = 0.06, MeOH); UV (MeOH) λ_{max} (log ε): 267.0 (5.56); ^{1}H NMR (400 MHz, $CDCl_3$) and ^{13}C NMR (100 MHz, $CDCl_3$): see SI Table S2; HR ESI-MS (*m/z*): 273.1851 $[M+H]^+$ (calcd for $C_{18}H_{25}O_2$ 273.1849).

Compound **14**: White amorphous powder; $[\alpha]_D^{25}$= + 60° (*c* = 0.12, MeOH); UV (MeOH) λ_{max} (log ε): 209 (4.63), 267 (4.64), 360 (3.56); ^{1}H NMR (400 MHz, $CDCl_3$) and ^{13}C NMR (100 MHz, $CDCl_3$): see SI Table S2; HR ESI-MS (*m/z*): 347.1856 $[M+H]^+$ (calcd for $C_{20}H_{27}O_5$ 347.1853).

Compound **15**: White amorphous powder; $[\alpha]_D^{25}$= + 39° (*c* = 0.08, MeOH); UV (MeOH) λ_{max} (log ε):

208 (4.47), 254 (4.38), 291 (4.22); ^{1}H NMR (400 MHz, CD_3OD) and ^{13}C NMR (100 MHz, CD_3OD): see SI Table S3; HR ESI-MS (*m/z*): 305.1753 $[M+H]^+$ (calcd for $C_{18}H_{25}O_4$ 305.1747).

Compounds **16** and **17**: Colorless solid; $[\alpha]_D^{25}$= 0° (*c* = 0.08, MeOH); ^{1}H NMR (400 MHz, $CDCl_3$) and ^{13}C NMR (100 MHz, $CDCl_3$): see SI Table S3; HR ESI-MS (*m/z*): 347.1855 $[M+H]^+$ (calcd. for $C_{20}H_{27}O_5$ 347.1853).

2. SI Results

2.1. Structure elucidation

Analysis of HR ESI-MS of **8** revealed that the molecular weight of **8** is 185.1173 (calcd. for $C_{10}H_{17}O_3$ 185.1172). The ^{1}H NMR spectrum of **8** (SI Table S2) showed one methyl group [δ_H 1.13 (3H, d, *J* = 6.4 Hz)], three methylene protons [δ_H 2.10-2.30], one methine proton [δ_H 3.73 (tq, 1H, *J* = 6.4 Hz)], and four olefinic protons [δ_H 5.51 (1H, dt, *J* = 15.2, 5.6 Hz), 5.53 (1H, dt, *J* = 15.2, 5.6 Hz), 5.80 (1H, dt, *J* = 16.0, 6.4 Hz), and 6.93 (1H, d, *J* = 16.0 Hz)]. The 9-hydroxydeca-2,6-dienoic acid moiety was further supported by the 2D NMR spectra of the compound (SI Figures S10-S12). The configurations of the two double bonds were determined as *E* based on the *J* values. Since the absolute configuration of C-9 can be deduced as *R* from the biosynthetic origin of 9-OH, which resulted from the reduction of a ketone group by the CcRadS1 KR domain,[2] C-11 was also determined to have an *R* configuration. Thus, the structure of compound **8** was established as (9*R*)-hydroxy-deca-(2*E*,6*E)*-dienoic acid.

Compounds **11** and **10** were homologs as shown by their similar UV absorption (SI Fig. S2) and as further evidenced by HR MS analysis (Compounds **11** and **10** molecular formulas are $C_{17}H_{24}O_4$ and $C_{19}H_{28}O_4$, respectively). Based on the homology of **11** to **10**, the structure of **11** was established as 2,4-dihydroxy-3-methyl-6-(2-oxononyl) benzaldehyde. The HR ESI-MS data were in agreement with the published data for **11**.[13]

Compound **13** has the same 4,6-dimethyl-octa-2,4-dien-1-one moiety as **12** based on comparison of the 1D and 2D NMR spectra of the two compounds. The ^{1}H NMR and ^{13}C NMR spectra showed the presence of a phenyl group and a -CH_2-CH_2-O- moiety. The connectivity of these three groups was

elucidated using the HMBC spectrum (SI Fig. S28). Based on foregoing evidence, the structure of **13** was established as phenethyl-4,6-dimethyl-octa-(2*E*,4*E*)-dienoate.

Compound **14** was obtained as a white amorphous powder, and its molecular formula was determined to be $C_{20}H_{26}O_5$ by HR ESI-MS. The ^{1}H NMR spectrum (SI Table S2) showed four methyl groups [δ_H 0.84 (t, *J* = 7.2 Hz), 0.99 (d, *J* = 6.4 Hz), 1.23 (t, *J* = 7.2 Hz), and 1.78 (d, *J* = 0.8 Hz)], three methylenes [δ_H 1.41 and 1.30 (each 1H, m), 4.15 (2H, s), and 4.25 (2H, q, *J* = 7.2 Hz)], one methine proton [δ_H 2.46 (1H, m)], three olefinic protons [δ_H 7.29 (d, *J* = 15.6 Hz), 6.14 (d, *J* = 15.6 Hz), and 5.75 (d, *J* = 9.6 Hz)], and two aromatic protons [δ_H 6.11 (d, *J* = 2.5 Hz), and 6.29 (d, *J* = 2.5 Hz)]. The 4,6-dimethyl-octa-2,4-dien-1-one moiety was further evidenced by ^{13}C NMR, ^{1}H-^{1}H COSY, and comparison with published data[9,14]. The rest of the structure was elucidated using HMBC data (SI Fig. S34). The correlations between H-8/C-9 and H-8/C-7 showed that the 4,6-dimethyl-octa-2,4-dien-1-one moiety was attached to C-8, and C-8 was attached to C-7, respectively. The ethoxy connected to C-1 was evidenced by the HMBC correlation of H-19/C-1. Thus, the structure of **14** was elucidated as ethyl-2,4-dihydroxy-6-[(3*E*, 5*E*)-5,7-dimethyl-2-oxo-5-nonadienyl]-benzoate.

Compound **15** was obtained as a white amorphous powder and its molecular formula was determined as $C_{18}H_{24}O_4$ by HR ESI-MS. Its aromatic ring is similar to that of **14** based on comparison of the NMR spectra of the two compounds (SI Tables S2 and S3). The 4,6-dimethyl-2,4-octadiene moiety was established by ^{1}H-NMR, ^{13}C-NMR and ^{1}H-^{1}H COSY data. This moiety was attached to C-7 as shown by the cross-peak between H-8 [δ_H 7.07 (d, *J* = 15.2 Hz)] and C-7 in the HMBC spectrum (SI Fig. S40). Compound **15** was therefore identified as ethyl-4,6-dihydroxy-6-[(1*E*,3*E*)-3,5-dimethylhepta-1,3-

dienyl]-benzoate.

The HR ESI-MS spectrum of **16/17** showed $[M+H]^+$ ion at (*m/z*): 347.1855 indicating a molecular formula of $C_{20}H_{26}O_5$. However, **16/17** was obtained as a mixture with two groups of signals (corresponding to **16** and **17**), with a peak area ratio of 1 : 0.7 by ^{1}H NMR.

The ^{1}H NMR spectroscopic data (SI Table S3) of **16** showed four methyl groups [δ_H 0.84 (t, *J* =7.2 Hz), 0.98 (d, *J* = 6.4 Hz), 1.24 (t, *J* = 7.2 Hz), and 1.80 (d, *J* = 0.8 Hz)], three methylenes [δ_H 1.38 and 1.29 (each 1H, m), 3.81 (2H, s), and 4.15 (2H, q, *J* = 7.2 Hz)], one methine proton [δ_H 2.50 (1H, m)], three olefinic protons [δ_H 7.35 (d, *J* = 15.2 Hz), 6.58 (d, *J* = 15.2 Hz), and 5.79 (d, *J* = 10.0 Hz)], and two aromatic protons [δ_H 6.33 (d, *J* = 1.6 Hz), and 6.32 (d, *J* = 1.6 Hz)]. Comparison of the NMR spectra of **16** and **14** (SI TablesS2 and S3) confirmed the presence of the same 4,6-dimethyl-octa-2,4-dien-1-one moiety in both compounds. The NMR spectra for the aromatic moiety of **16** are similar to those of 2-(2-decanoyl-3,5-dihydroxyphenyl) acetic acid, reported in our previously work.[2] Based on the above evidence, the structure of **16** was determined as ethyl-2-(2-[(2*E*,4*E*)-4,6-dimethylocta-2,4-dienoyl]-3,5-dihydroxyphenyl)-acetate.

The NMR data of **17** showed that its aromatic moiety was the same as that in **16**. However, differences in the NMR spectra for the C_3-C_6 region of **17** and **16** indicate that the double bond has a *Z* configuration in **17**. This was further evidenced by the 1D NOESY spectra, with H-4 showing a NOE effect with H-18 in for **17**, and H-4 having a NOE effect with H-6 for **16** (SI Fig. S3). Thus, the structure of **17** was elucidated as ethyl-2-(2-[(2*E*,4*Z*)-4,6-dimethylocta-2,4-dienoyl]-3,5-dihydroxyphenyl)-acetate.

2.2. Production of fatty acyl-primed compounds 10 and 11 by chimeric and native AfoE

In addition to pre-asperfuranone (**6**), *S. cerevisiae* expressing the AfoG - AfoE pair also produced two acyl benzaldehydes (ABHs) primed by medium-chain fatty acids (**10**, 0.13 mg/L and **11,** trace amounts, Figure 2). Compounds **10** and **11** were also produced by *S. cerevisiae* strains expressing AfoE alone, and those expressing AfoE-SAT_{BDLS} hybrids with or without the hrPKS partners (Fig. 2). To produce **10**, AfoE and its derivatives utilize a decanoyl fatty acid intermediate, and extend this substrate with four additional ketide units in a manner that maintains the native programming of AfoE as seen for the natural product pre-asperfuranone **6**. Compound **10** had previously been also isolated in small amounts from an *A. nidulans* strain upon *in situ* replacement of SAT_{AfoE} with the SAT domain of the *A. nidulans* nrPKS AN3386.[15,16] In its native context, AN3386 utilizes a decanoyl acyl chain biosynthesized by the medium chain fatty acid synthase AN3380 - AN3381 pair whose encoding genes are clustered with the gene for AN3386. The main products of the engineered *A. nidulans* strain expressing AfoE-SAT_{AN3386} are, however, acyl benzaldehyde (ABH) **18** in the mycelia, and pyrone **19** in the medium (Fig. S46)[15]. Both **18** and **19** feature a decanoyl starter unit that is extended by three ketide units, in an apparent sputtering by the chimeric AfoE-SAT_{AN3386}. Additional replacement of the KS-AT didomain (hence, AfoE-$[SAT+KS+AT]_{AN3386}$, referred to as Chimera B by Liu *et al.*[15]) is necessary to channel polyketide production towards **10** as the main product in *A. nidulans*. In contrast, we have not detected **18** or **19**, or indeed any other pyrone derailment products in our yeast strains that produced **10** and **11**. While the *A. nidulans* system[15] and our strains may have been expected to produce the same main products, it is

important to remember that the AfoE chimeras in these two studies were engineered using different SAT domains, utilized slightly different artificial domain junctures, and were expressed in different hosts. We speculate that production of **18** and **19** in *A. nidulans* expressing AfoE-SAT_{AN3386} indicates an ample supply of the decanoyl fatty acid intermediate loaded to the enzyme. At the same time, polyketide extension may have been slowed by a suboptimal protein interaction with the foreign SAT domain, leading to the off-loading of the partially extended derailment product by the reductive release (R) domain (as in the case of **18**), or spontaneous release of a stalled intermediate (as for the pyrone **19**). For the yeast system in our experiments, the supply of the decanoyl fatty acyl intermediate is more limited, considering that this originates from the primary metabolism of the yeast host, and its production does not benefit from a partner enzyme dedicated to its production (such as AN3380-3381). At the same time, chain extension on the native AfoE or the AfoE-SAT_{BDLS} chimeras is sufficiently fast to allow the formation of **10** as the main product. Expression of AfoE-SAT_{AN3386} in yeast, and conversely, expression of a representative AfoE-SAT_{BDLS} hybrid in *A. nidulans* may help to elucidate the control of these interesting quantitative differences in product formation in the two heterologous ABH production systems.

3. SI Tables

Table S1. PCR primers used in this study

Primer Name (Restriciton site)	Primer Sequence (5' – 3')	Product (Size in kb)
AfoG_1_F (*Nde*I)	CTCGAGTTTTTCAGCAAGATCATATGGGCAGCACATCTTCCG	AfoG fragment 1
AfoG_1_R	TGCCCCTTTGACATGCGTCGTCCCCAGCTTCTCACTATC	(0.3)
AfoG_2_F	ACGCATGTCAAAGGGGCACATTTTC	AfoG fragment 2
AfoG_2_R	AATTGCGGATCGAGGGTAGCAGCTGTCTCCGCCGAAT	(0.1)
AfoG_3_F	ACCCTCGATCCGCAATTCCGC	AfoG fragment 3
AfoG_3_R	TGGATGGAATCGTCAGGCCAGCATTTTCAAGAGCCTCATAGAC	(0.1)
AfoG_4_1_F	CTGGCCTGACGATTCCATCCATC	AfoG fragment 4
AfoG_4_1_R	CTCGCAATTGGCTCCATGTGGTGCGAGTGATATCCCGT	(2.0)
AfoG_4_2_F	ACCACATGGAGCCAATTGCGAGC	AfoG fragment 5
AfoG_4_2_R (*Pme*I)	AGGAGATCTTCTAGAAAGATGTTTAAACTCAAGCAACAACGACAGTTC	(5.6)
AfoE_1_F (*Nde*I)	CTCGAGTTTTTCAGCAAGATCATATGACCCGAGCAAGCGCC	AfoE fragment 1
AfoE_1_R	GATCGAGCTGAATGCACGGTAGACATTGCGGCCCTGC	(4.7)
AfoE_2_F	CCGTGCATTCAGCTCGATCGTCG	AfoE fragment 2
AfoE_2_R	TGACCGACAGGATTGTCCATGTGGTACACTGGGTATGCCTC	(3.3)
AfoE_3_F	ACCACATGGACAATCCTGTCGGTCAG	AfoE fragment 3

AfoE_3_R (*Pme*I)	AGGAGATCTTCTAGAAAGATGTTTAAACTCAGGCGAGGTAGCCCAT	(0.4)
AfoC_F (*Nde*I)	CATCATATGCCGGCGCTCGATATC	AfoC
AfoC_R (*Pme*I)	CGGGTTTAAACTCAACATCTCAAGCTTTC	(0.8)
AfoESAT_ResS2_F (*Nde*I)	ATTCATATGACCCGAGCAAGCGCCTC	AzResS2-SAT$_{AfoE}$
AfoESAT_ResS2_R	GATGTCTGAGGCACCTGGCCCGGTTGAAGCTGGGGTTGT	fragment 1 (1.3)
ResS2_AfoESAT_Dn_F	GGCCAGGTGCCTCAGACATCCC	AzResS2-SAT$_{AfoE}$
ResS2_AfoESAT_Dn_R	ACTCATGCACGCCAGGTGGATGG	fragment 2 (0.6)
(*Sex*A1)		
AfoESAT_ResS2_F (*Nde*I)	ATTCATATGACCCGAGCAAGCGCCTC	LtlasS2-SAT$_{AfoE}$
AfoESAT_LasS2_R	GTCTGGGCCGGGGAGCTTTGTCGGTTGAAGCTGGGGTTGT	fragment 1 (1.3)
LasS2_AfoESAT_Dn_F	ACAAAGCTCCCCGGCCCAGAC	LtLasS2-SAT$_{AfoE}$
LasS2_AfoESAT_Dn_R (*Blp*I)	ACGCCGGATTTGCTGAGGCAG	fragment 2 (0.7)
AfoESAT_CurS2_F (*Not*I)	AACAAAAGCTGGAGCTCGGATCC	AtCurS2-SAT$_{AfoE}$
AfoESAT_CurS2_R	TGGCTCGACGCGGGTGGTCT	fragment 1 (1.9)
CurS2_AfoESAT_Dn_F	AGACCACCCGCGTCGAGCCAAAGCCACCAACCCCAGACAGT	LtLasS2-SAT$_{AfoE}$
CurS2_AfoESAT_Dn_R	TATCGCCCACCTGGGTTCCC	fragment 2 (1.0)
(*Bsu*36I)		
AfoESAT_RadS2_F (*Nde*I)	ATTCAT ATGACCCGAGCAAGCGCCTC	CcRadS2-SAT$_{AfoE}$
AfoESAT_RadS2_R	ATGTTGATACCGAGGCCTGCGGTTGAAGCTGGGGTTGTG	fragment 1 (1.3)
RadS2_AfoESAT_Dn_F	CAGGCCTCGGTATCAACATCATCATC	CcRadS2-SAT$_{AfoE}$

RadS2_AfoESAT_Dn_R (*Age*I)	ATCAACTCTTGGGTACTTGACGCAGTGC	fragment 2 (1.6)
RadS2SAT_AfoE_F (*Nde*I)	GGACTACAAAGACGATGACGACAAGCTTC	AfoE-SAT$_{CcRadS2}$
RadS2SAT_AfoE_R	GCTGCTGCTGCAGTTGCAGGACCGAGGCCTGAAGAAGGGAC	fragment 1 (1.2)
AfoE_RadS2SAT_Dn_F	GTCCTGCAACTGCAGCAGCAGC	AfoE-SAT$_{CcRadS2}$
AfoE_RadS2SAT_Dn_R	TCGTTTTGGTACACGGCGCTCG	fragment 2 (0.9)
(*Sex*AI)		
LasS2SAT_AfoE_F (*Not*I)	AGCTGGAGCTCGGATCCATTTAGCG	AfoE-SAT$_{LtLasS2}$
LasS2SAT_AfoE_R	TGCTGCTGCAGTTGCAGGACTTGTTCCAGGGAGTTGTCGT	fragment 1 (1.8)
AfoE_LasS2SAT_Dn_F	GTCCTGCAACTGCAGCAGCAGC	AfoE-SAT$_{LtLasS2}$
AfoE_LasS2SAT_Dn_R (*Sex*AI)	TCGTTTTGGTACACGGCGCTCG	fragment 2 (0.9)
ResS2SAT_AfoE_F (*Not*I)	AACAAAAGCTGGAGCTCGGATCC	AfoE-SAT$_{AzResS2}$
ResS2SAT_AfoE_R	ATCTGTCTCTGCCTGTGCATGGGC	fragment 1 (1.8)
AfoE_ResS2SAT_Dn_F	ATGCACAGGCAGAGACAGATGTCATGCCCGTCTCGCCCC	AfoE-SAT$_{AzResS2}$
AfoE_ResS2SAT_Dn_R (*Spe*I)	AGCTCCGTTGGCCTCGGACAG	fragment 2 (2.1)
CurS2SAT_AfoE_F (*Not*I)	AACAAAAGCTGGAGCTCGGATCC	AfoE-SAT$_{AtCurS2}$
CurS2SAT_AfoE_R	CGCAGTGATCCTATCCTGGAGGG	fragment 1 (1.7)
AfoE_CurS2SAT_Dn_F	TCCAGGATAGGATCACTGCGGTCATGCCCGTCTCGCCCC	AfoE-SAT$_{AtCurS2}$
AfoE_CurS2SAT_Dn_R (*Spe*I)	AGCTCCGTTGGCCTCGGACAG	fragment 2 (2.1)

Table S2. ^{1}H NMR (400 MHz) and ^{13}C NMR (100 MHz) data of compounds 8, 13, and 14 (δ in ppm, J in Hz).

No.	**8** (CD_3OD)		**13** ($CDCl_3$)		**14** ($CDCl_3$)	
	δ_C	δ_H	δ_C	δ_H	δ_C	δ_H
1	170.3		167.7		170.7	
2	123.1	5.80 (1H, d, 16.0)	115.5	5.75 (1H, d, 15.6)	105.6	
3	150.6	6.93 (1H, dt, 16.0, 6.4)	150.4	7.29 (1H, d, 15.6)	165.6	
4	33.2	2.31 (2H, dt, 14.4, 6.4)	131.7		103.0	6.29 (1H,d,2.5)
5	32.4	2.20 (1H, m)	148.8	5.64 (1H, d, 9.6)	160.8	
6	132.6	5.51 (1H,dt, 15.4, 5.6)	35.2	2.42 (1H, m)	113.1	6.11 (1H, d, 2.5)
7	131.6	5.53 (1H, dt, 15.4, 5.6)	30.2	1.39 (1H, m),1.29 (1H, m)	139.3	
8	43.5	2.16 (1H, m), 2.10 (1H, m)	12.1	0.82 (3H, t, 7.6)	49.1	4.15 (2H, s)
9	68.7	3.73 (1H, tq, 6.4)	20.3	0.96 (3H, d, 6.4)	198.0	
10	23.0	1.13 (3H, d, 6.4)	12.6	1.75 (3H, d, 1.2)	123.1	6.14 (1H, d, 15.6)
11			138.2		148.8	7.29 (1H, d, 15.6)
12			129.1	7.28 (2H, d, 8.0)	131.8	
13			128.7	7.21 (2H, br t, 8.0)	150.4	5.75 (1H, d, 9.6)
14			126.7	7.23 (1H, br d, 8.0)	35.1	2.46 (1H, m)
15			35.4	2.97 (2H, d, 6.4)	30.0	1.41 (1H, m), 1.30 (1H, m)
16			64.9	4.35 (2H, d, 6.4)	11.9	0.84 (3H, t, 7.2)
17					20.1	0.99 (3H, d, 6.4)
18					12.5	1.78 (3H, d, 0.8)
19					61.4	4.25 (2H, q, 7.2)
20					14.1	1.23 (3H, t, 7.2)
3-OH						11.7 (1H, s)

Table S3. ^{1}H NMR (400 MHz) and ^{13}C NMR (100 MHz) data of compounds 15, 16, and 17 (δ in ppm, J in Hz).

No.	15 (CD_3OD)		16 ($CDCl_3$)		17 ($CDCl_3$)	
	δ_C	δ_H	δ_C	δ_H	δ_C	δ_H
1	172.8		171.0		171.0	
2	131.0		40.9	3.81 (2H,s)	40.9	3.81 (2H,s)
3	165.6		136.7		136.7	
4	102.9	6.20 (1H, d, 2.4)	102.7	6.33 (1H, d, 1.6)	102.7	6.33 (1H, d, 1.6)
5	160.8		164.0*		164.0*	
6	108.7	6.44 (1H, d, 2.4)	111.4	6.32 (1H, d, 1.6)	111.4	6.32 (1H, d,1.6)
7	144.9		164.1*		164.1*	
8	128.1	7.07 (1H, d, 15.2)	135.0		135.0	
9	137.2	6.50 (1H, d, 15.2)	195.2		195.2	
10	134.3		124.3	6.58(1H, d, 15.2)	126.4	6.67 (1H, d, 15.2)
11	141.8	5.38 (1H, d, 9.6)	149.7	7.35 (1H,d, 15.2)	140.9	7.79 (1H, d, 15.2)
12	35.9	2.48 (1H, m)	132.2		130.0	
13	31.7	1.33 (1H, m), 1.28 (1H, m)	151.2	5.79(1H, d, 10.0)	148.6	5.62 (1H, d, 10.0)
14	12.5	0.89 (3H, t, 7.2)	34.1	2.50 (1H,m)	35.2	2.70 (1H, m)
15	21.2	1.00 (3H, d, 6.4)	30.1	1.38 (1H,m), 1.29 (1H,m)	30.1	1.38 (1H, m), 1.29 (1H,m)
16	13.3	1.87 (3H, d, 1.2)	11.9	0.84 (3H, t, 7.2)	11.9	0.84 (3H, t, 7.2)
17	62.5	4.25 (2H, q, 7.0)	20.1	0.98 (3H, d, 6.4)	20.8	0.98 (3H, d, 6.4)
18	14.9	1.40 (3H, t, 7.0)	12.4	1.80 (3H, d, 1.2)	20.1	1.87 (3H, d, 0.8)
19			61.4	4.15 (2H, q, 7.2)	61.4	4.15 (2H, q, 7.2)
20			29.9	1.24 (3H, t, 7.2)	29.9	1.24 (3H, t, 7.2)

* Signals may be interchanged.

4. SI Figures

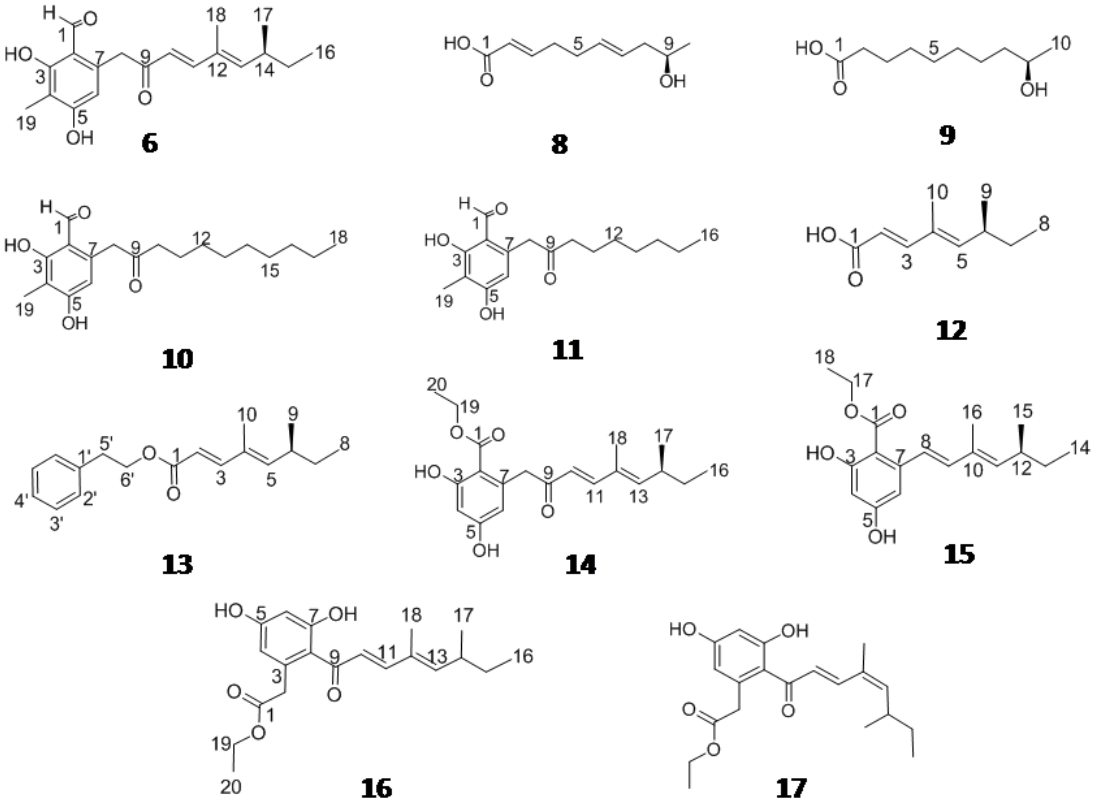

Figure S1. The chemical structures of compounds 6 and 8-17

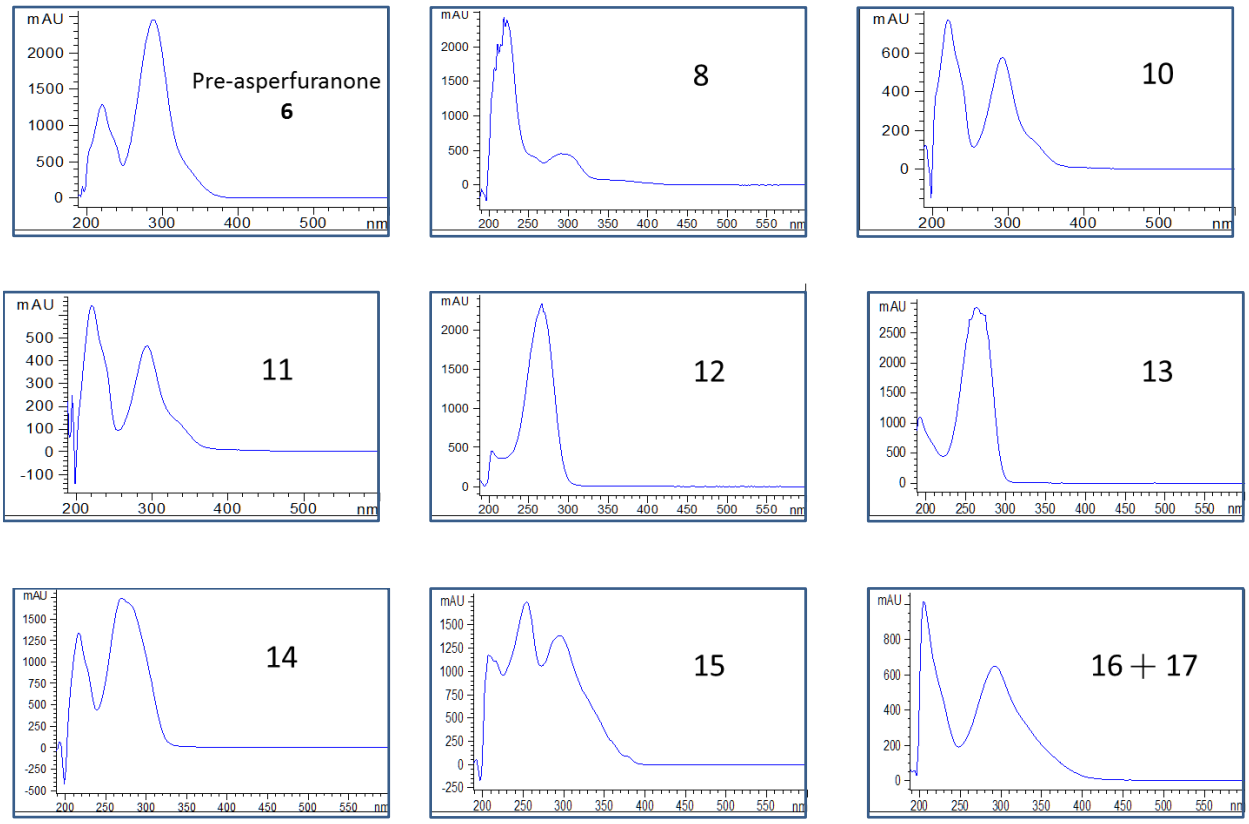

Figure S2. The UV absorption spectra of compounds 6, 8, and 10-17

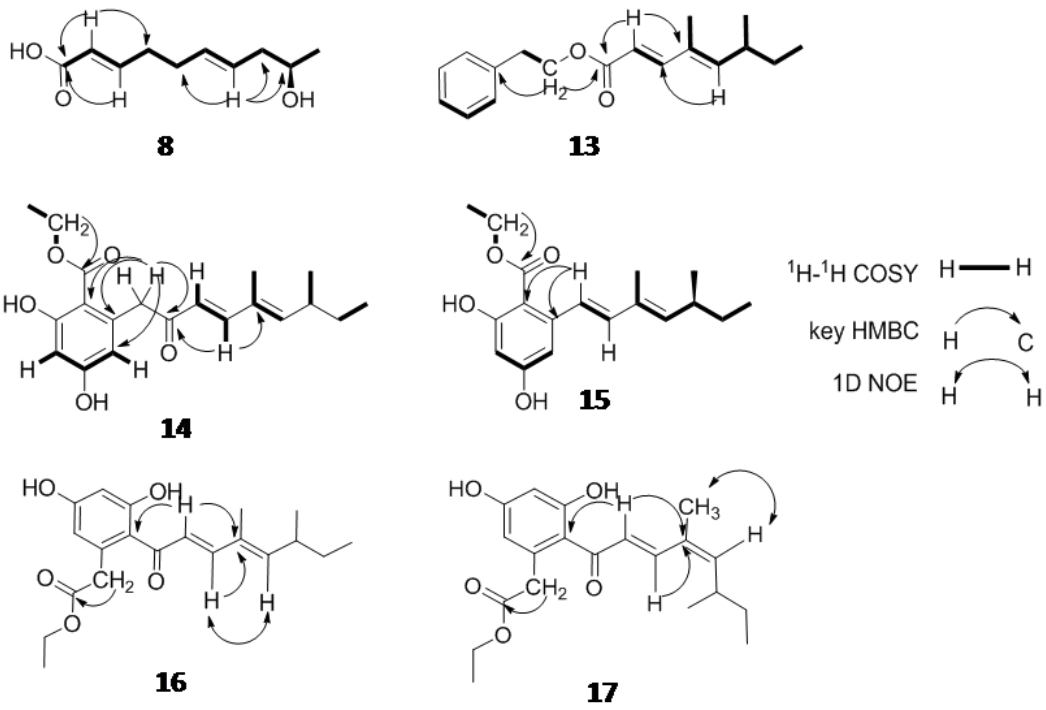

Figure S3. Key HMBC (→), 1H-1H-COSY (—) and 1D NOE (←→) correlations for compounds 8 and 13-17

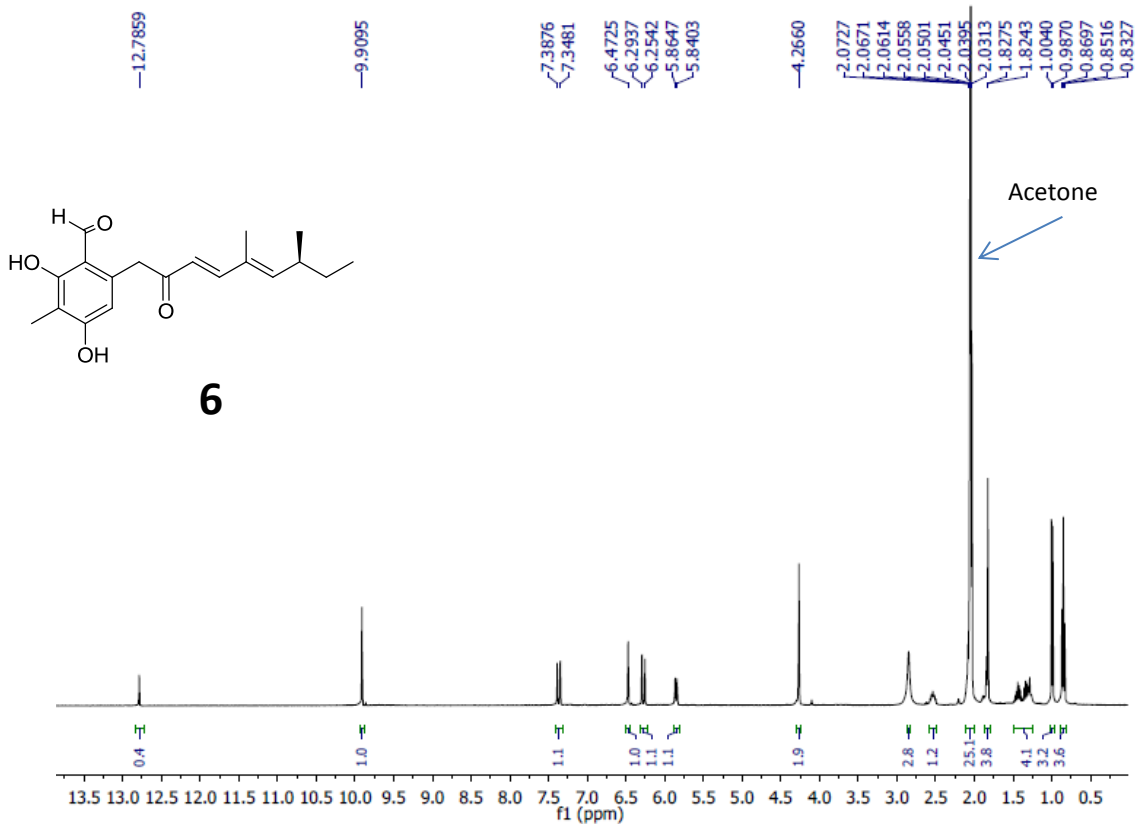

Figure S4. ^{1}H NMR Spectrum (400 MHz) of Pre-asperfuranone (6) in CD_3COCD_3

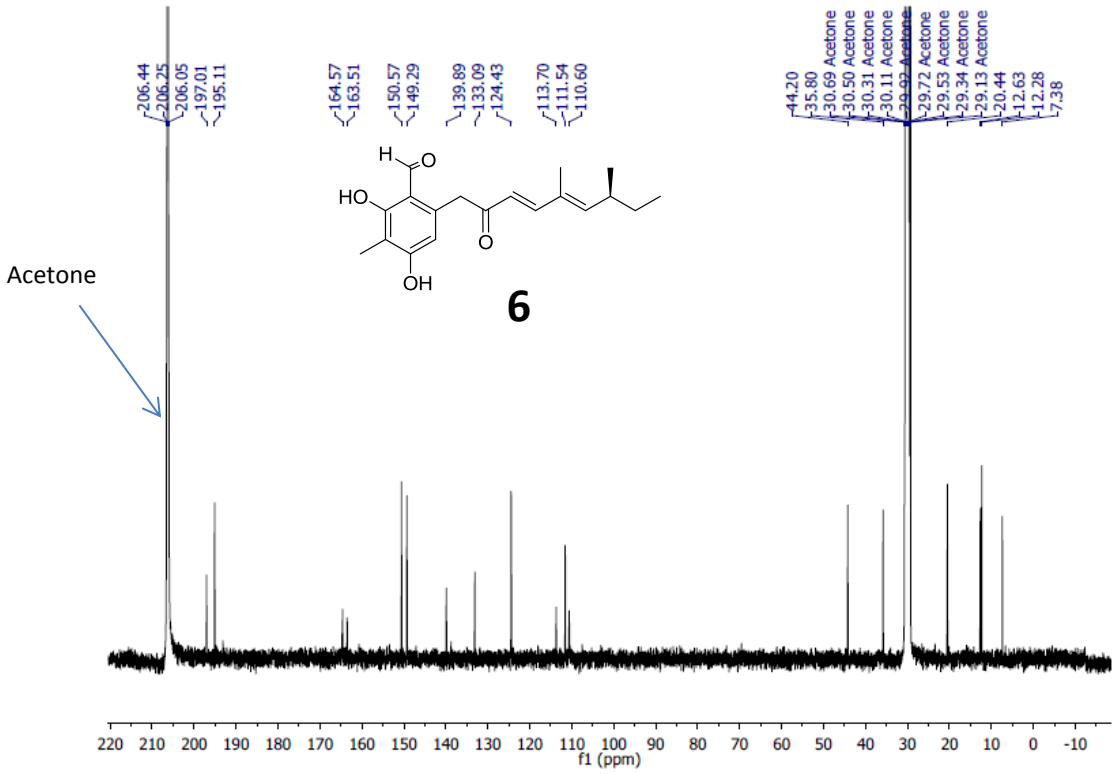

Figure S5. ^{13}C NMR Spectrum (100 MHz) of Pre-asperfuranone (6) in CD_3COCD_3

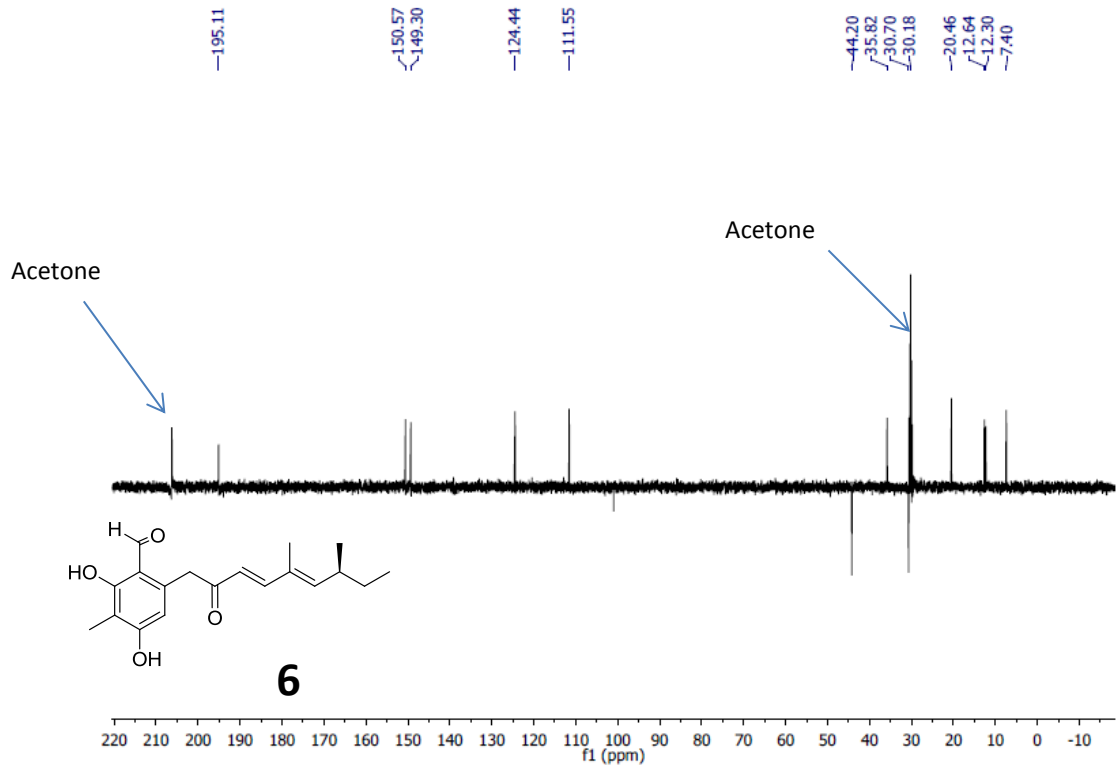

Figure S6. DEPT135 spectrum (100 MHz) of Pre-asperfuranone (6) in CD_3COCD_3

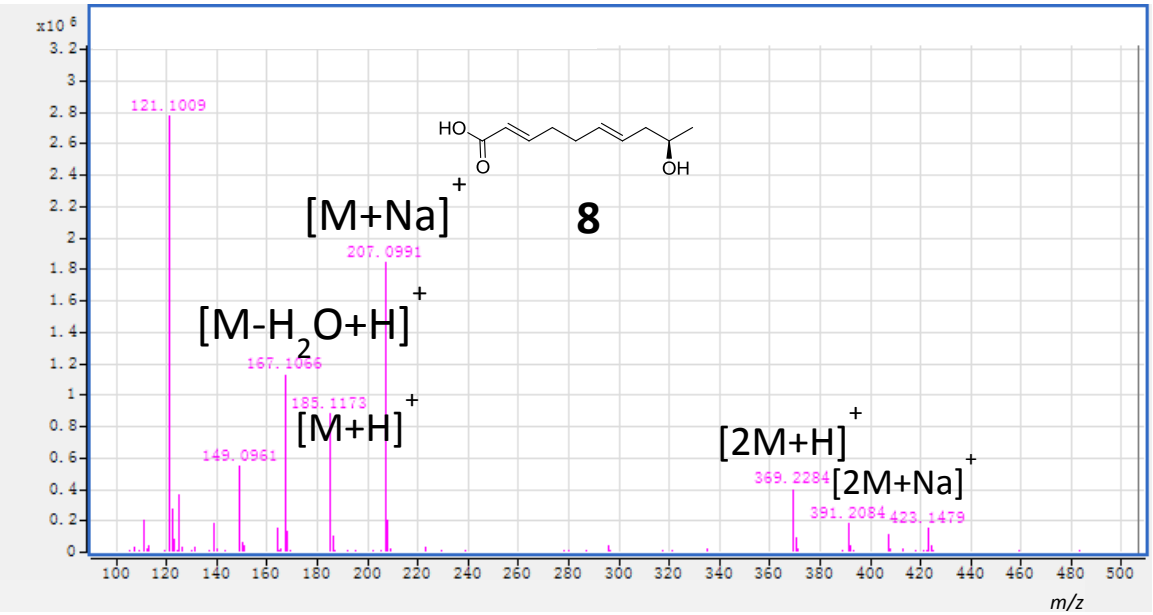

Figure S7. HR ESI-MS of Compound 8

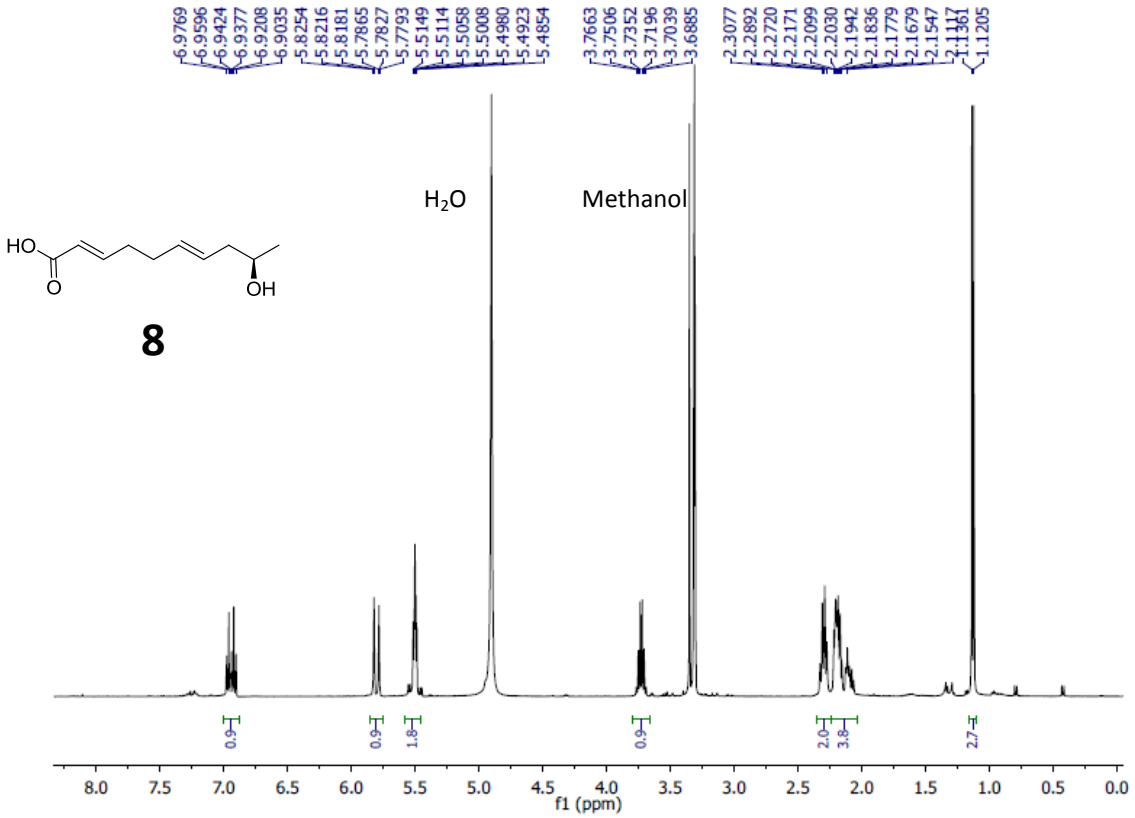

Figure S8. ^{1}H NMR Spectrum (400 MHz) of Compound 8 in CD_3OD

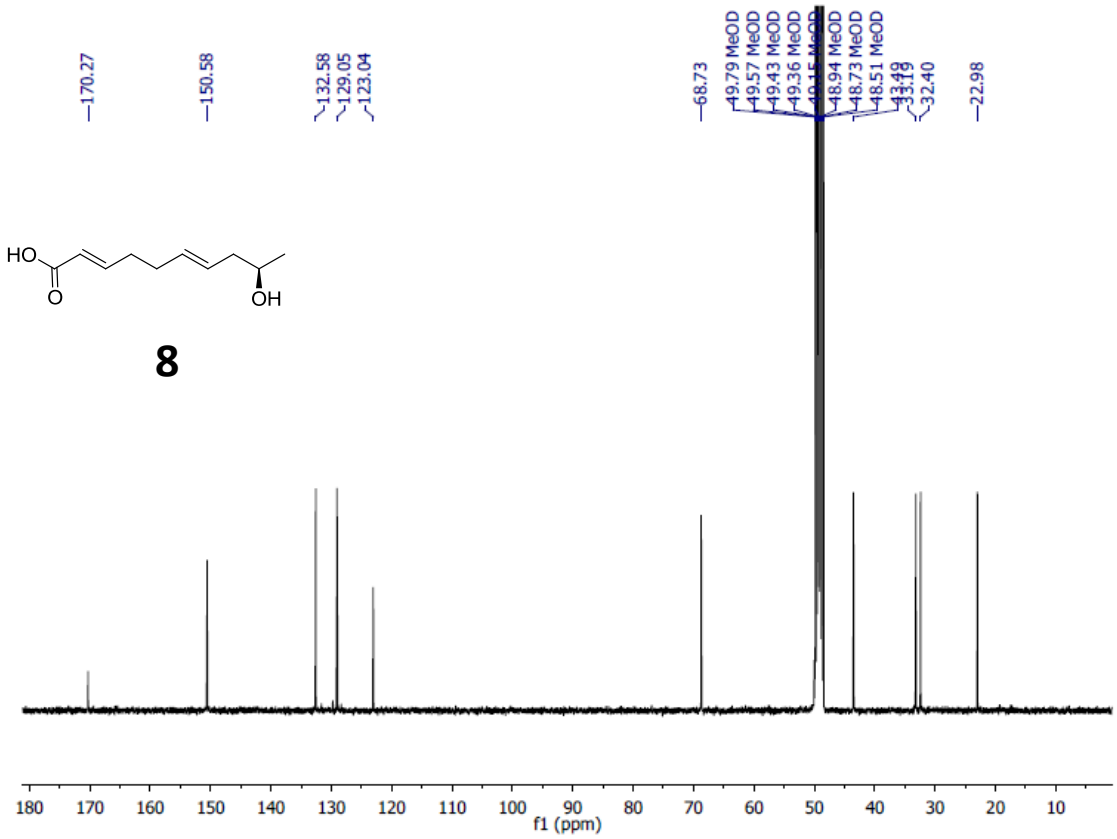

Figure S9. ^{13}C NMR Spectrum (100 MHz) of Compound 8 in CD_3OD

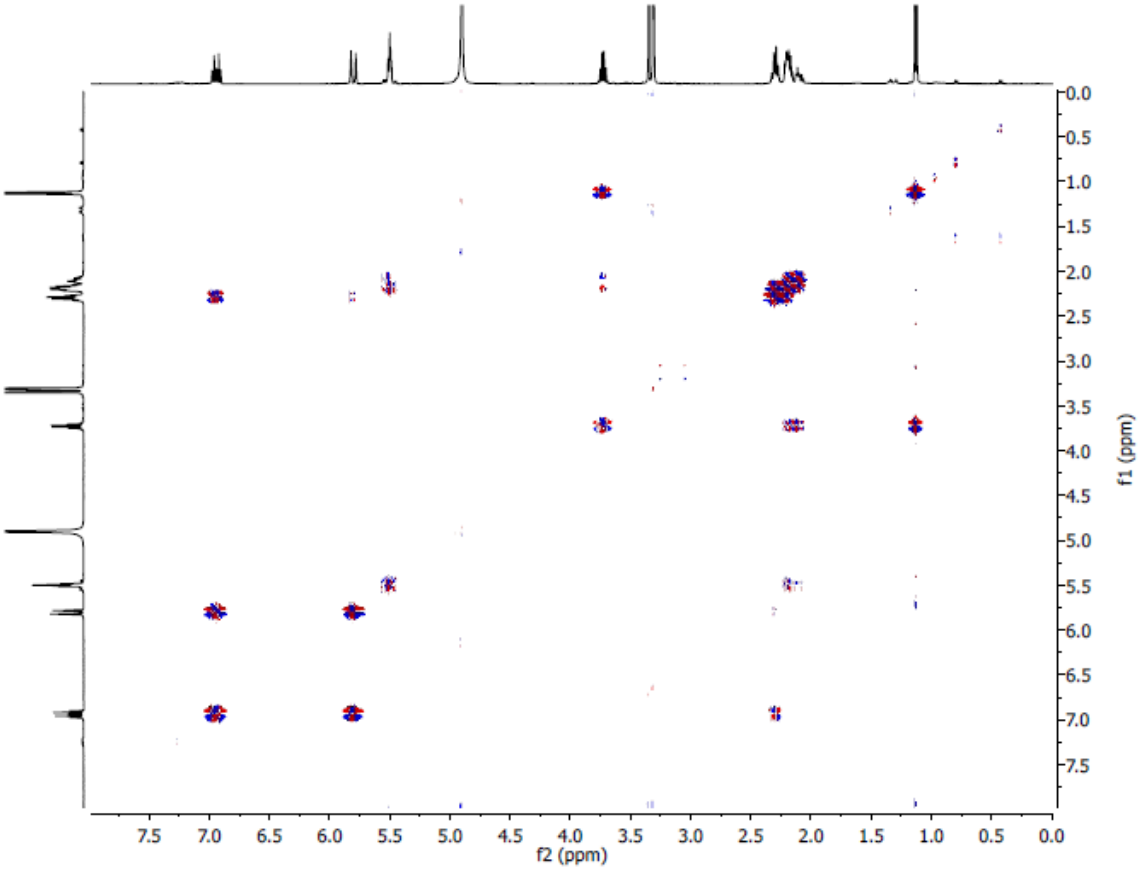

Figure S10. ^{1}H-^{1}H COSY Spectrum (400 MHz) of Compound 8 in CD_3OD

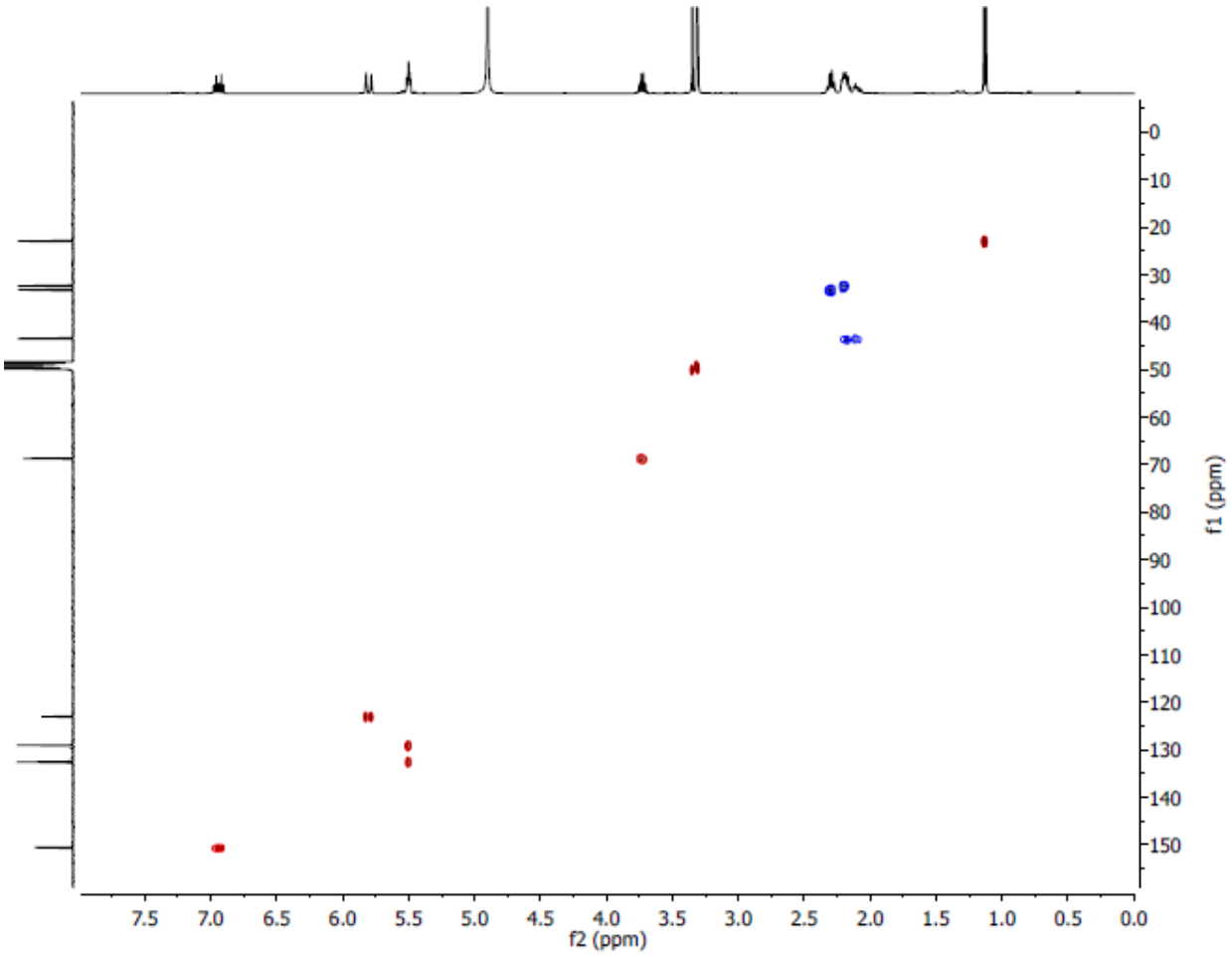

Figure S11. HSQC Spectrum (400 MHz) of Compound 8 in CD_3OD

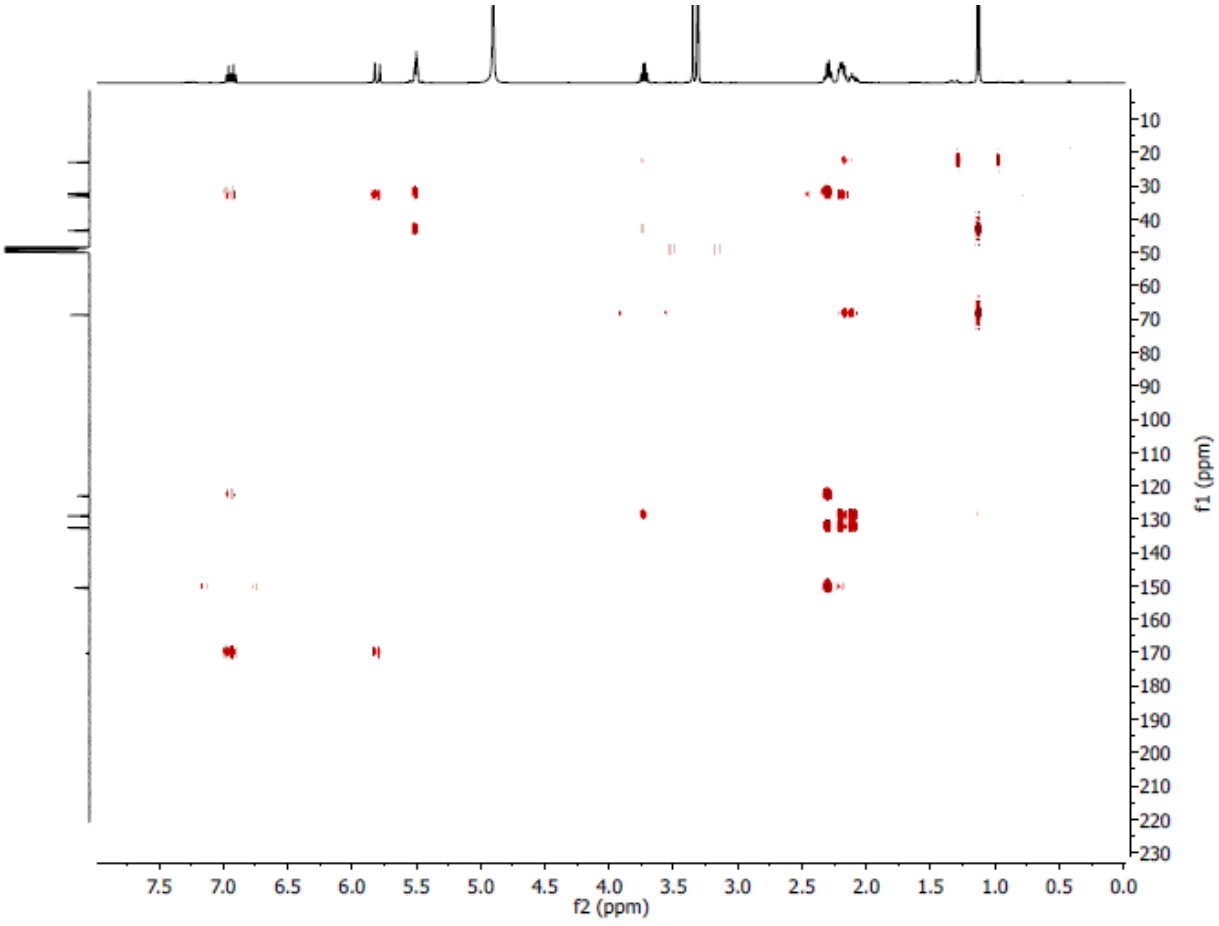

Figure S12. HMBC Spectrum (400 MHz) of Compound 8 in CD_3OD

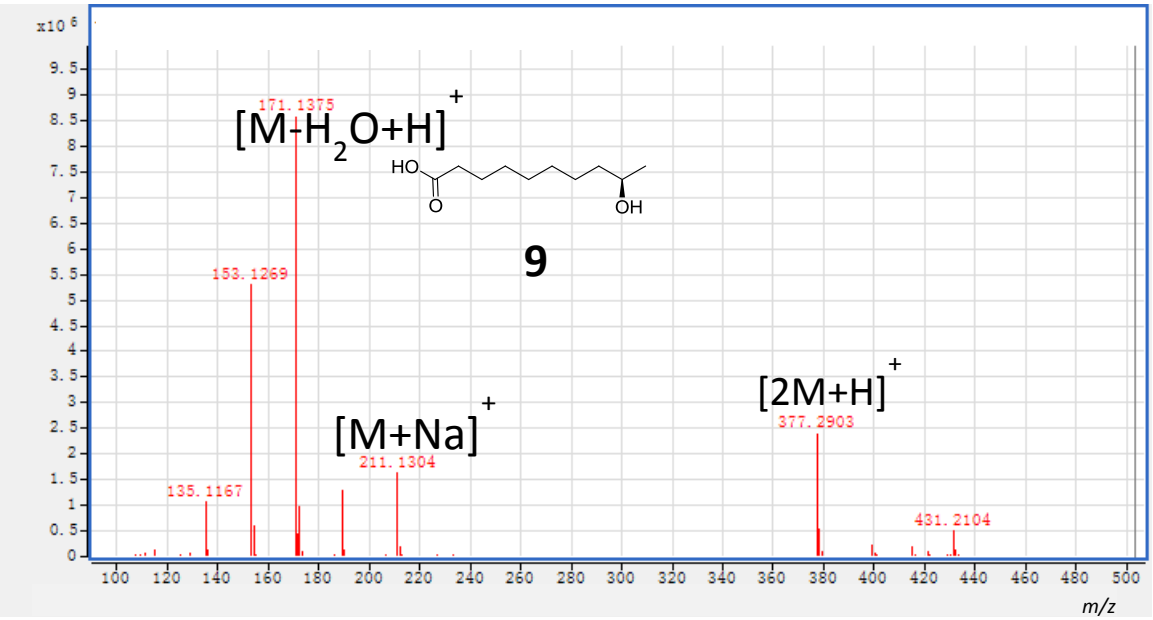

Figure S13. HR ESI-MS of Compound 9

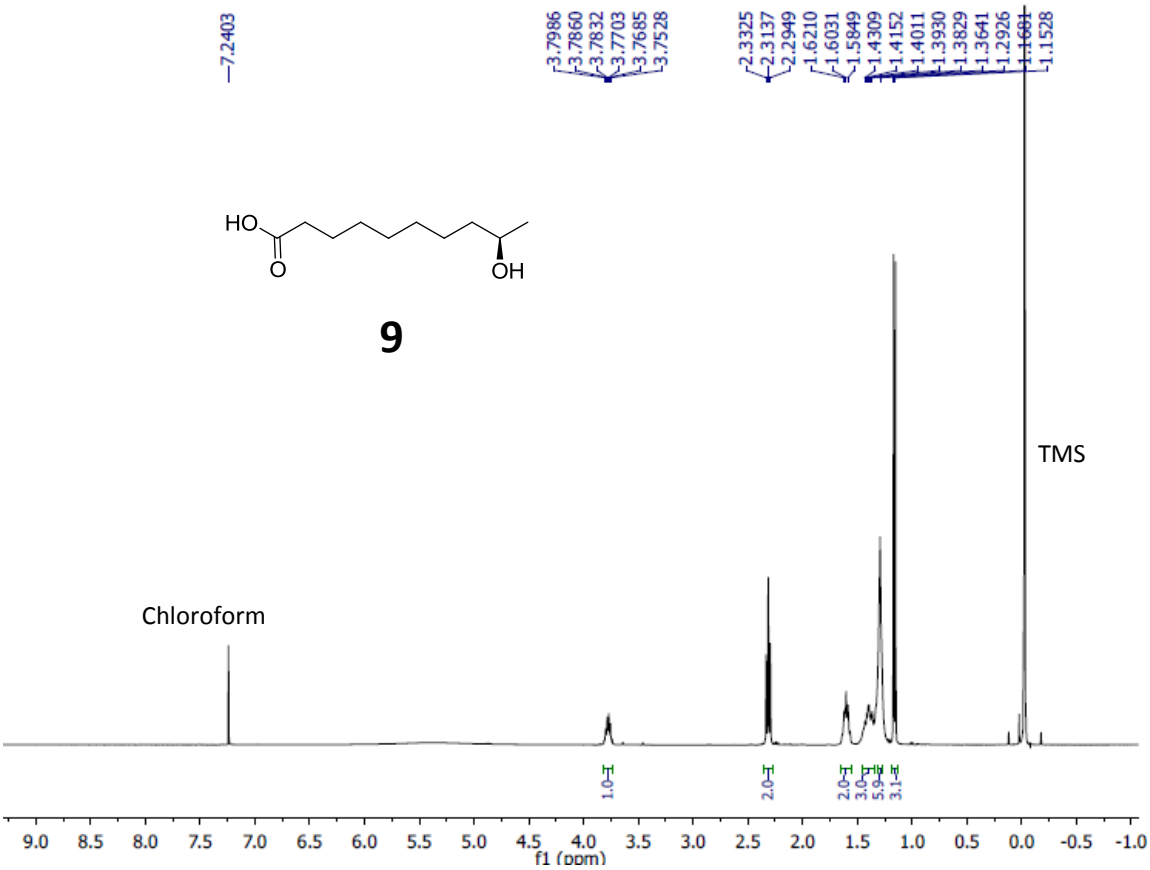

Figure S14. ^{1}H NMR Spectrum (400 MHz) of Compound 9 in $CDCl_3$

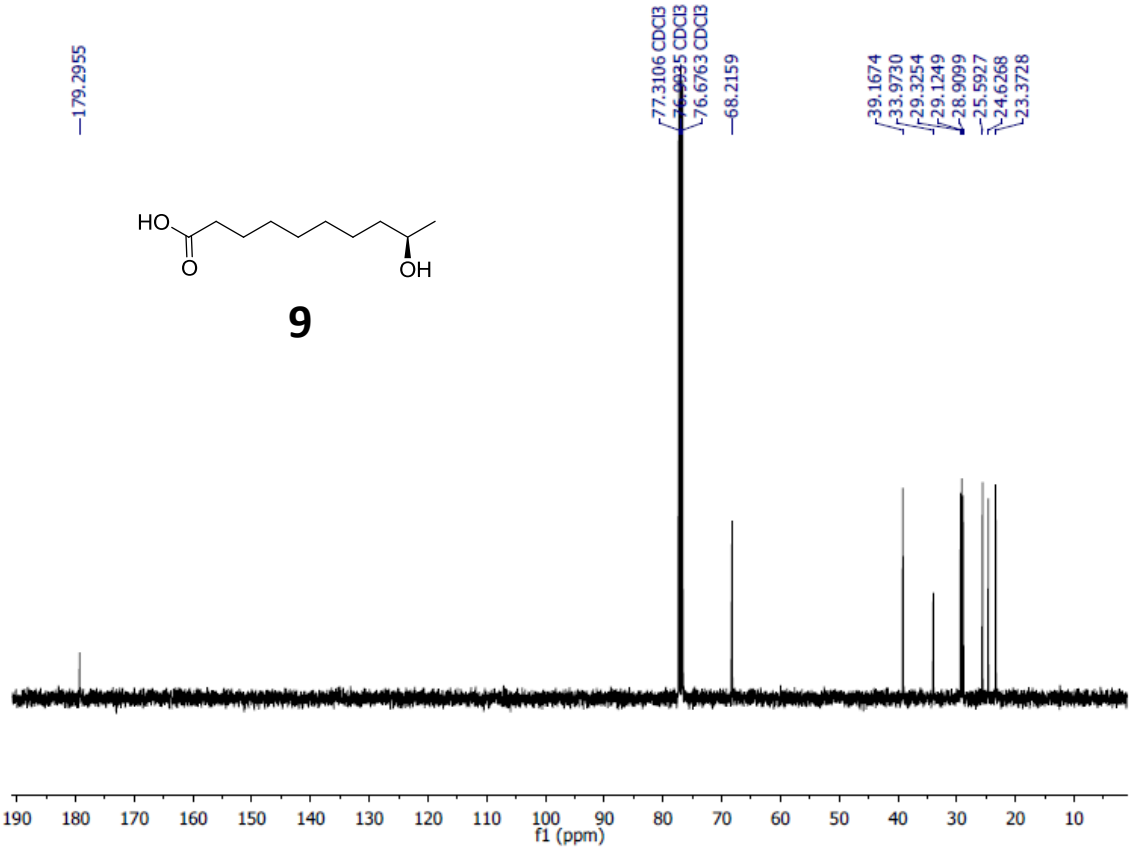

Figure S15. ^{13}C NMR Spectrum (100 MHz) of Compound 9 in $CDCl_3$.

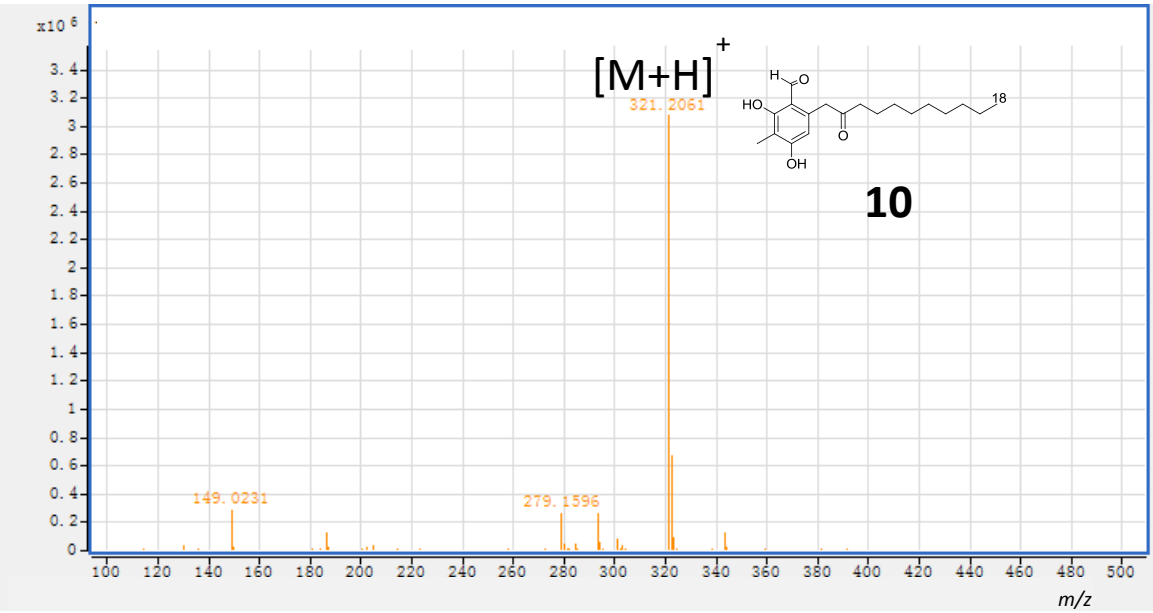

Figure S16. HR ESI-MS of Compound 10.

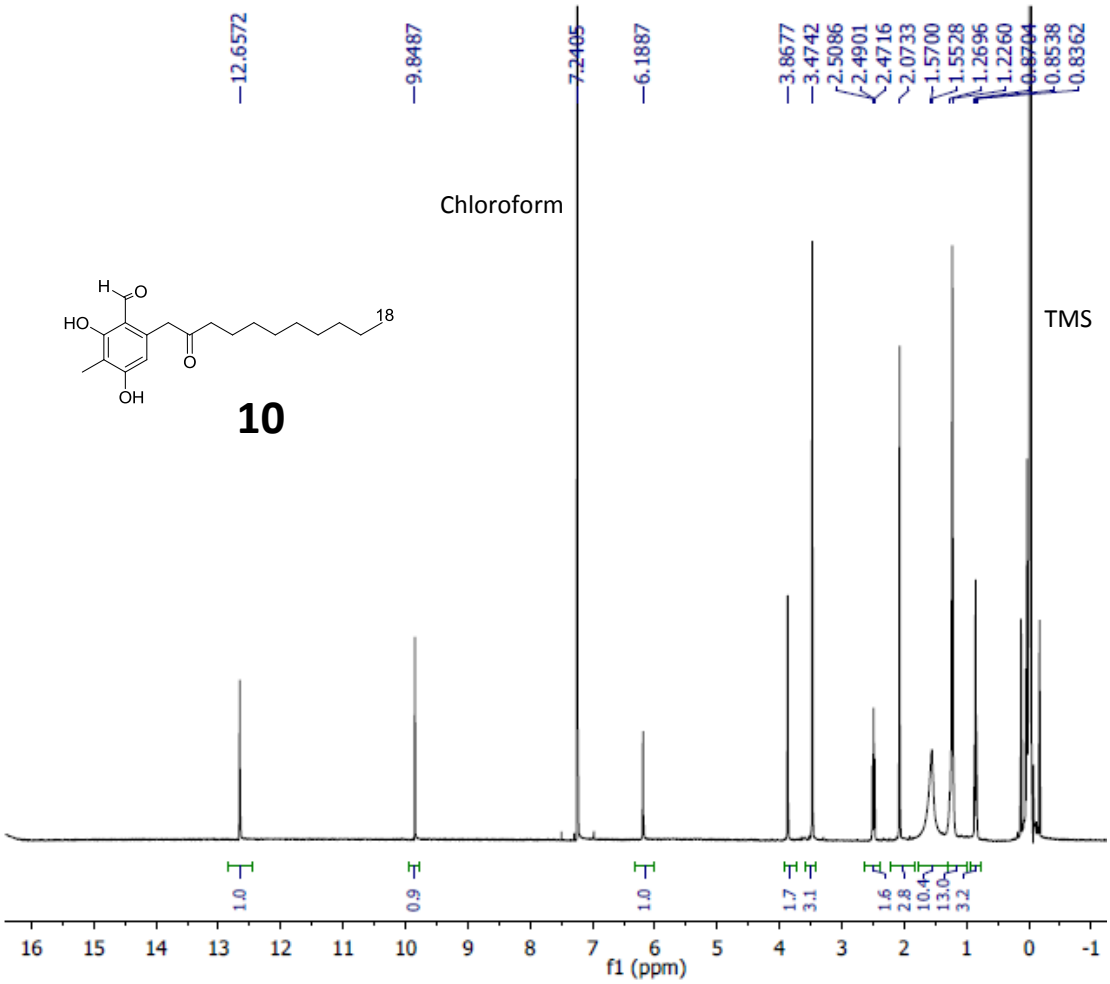

Figure S17. ^{1}H NMR Spectrum (400 MHz) of Compound 10 in $CDCl_3$.

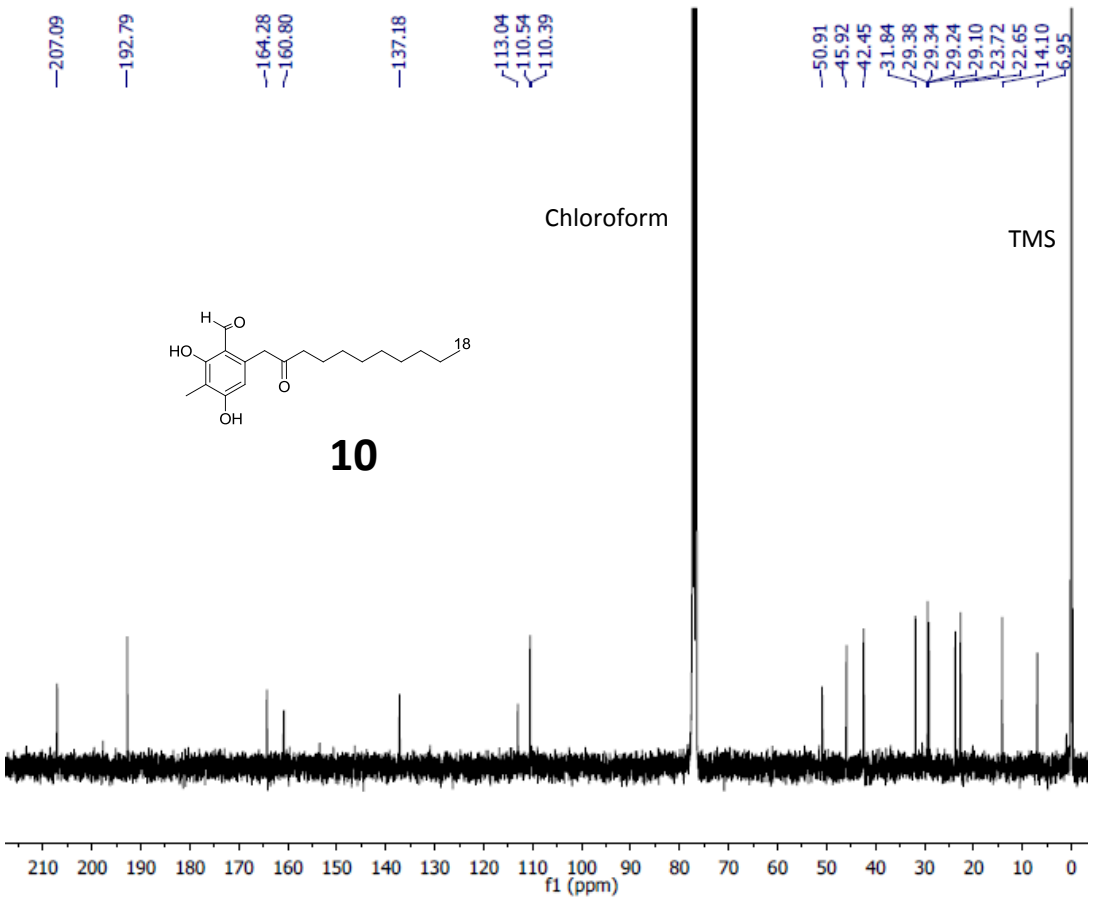

Figure S18. ^{13}C NMR Spectrum (100 MHz) of Compound 10 in $CDCl_3$.

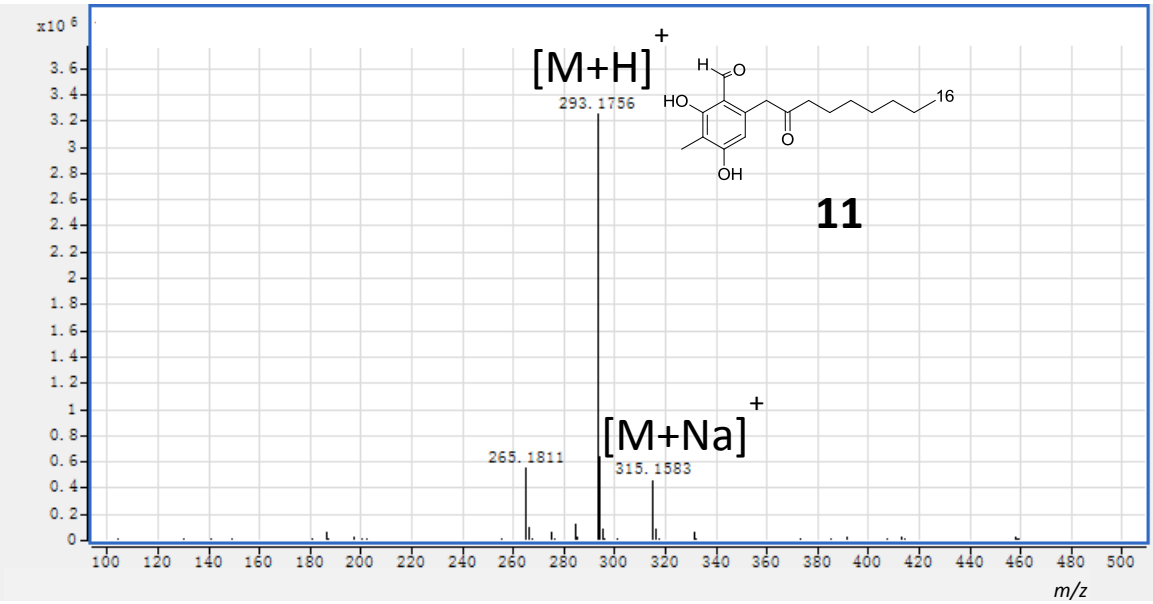

Figure S19. HR ESI-MS of Compound 11.

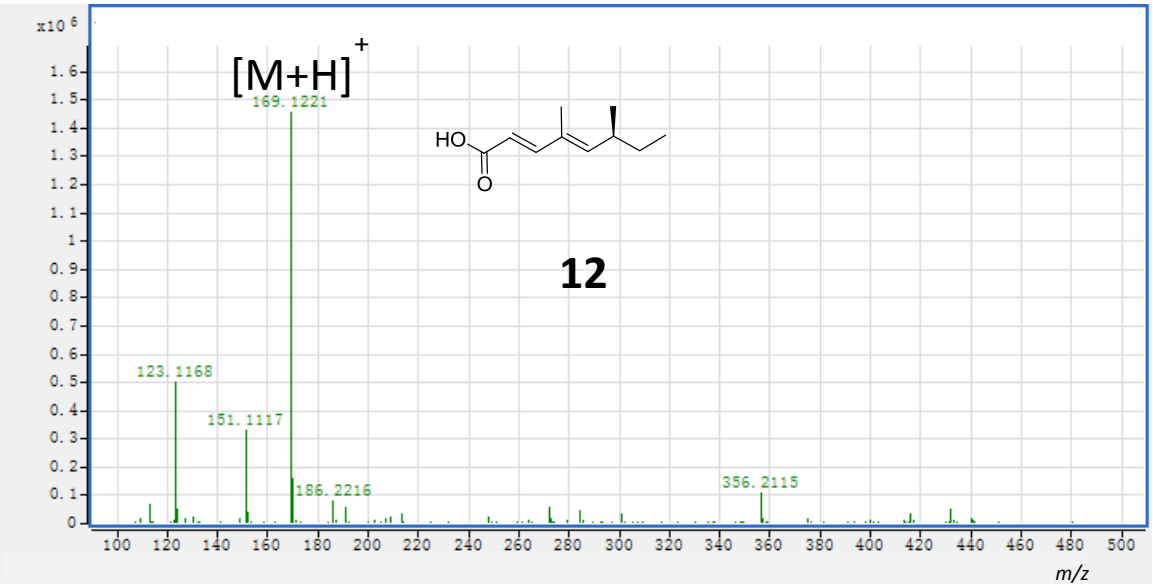

Figure S20. HR ESI-MS of Compound 12.

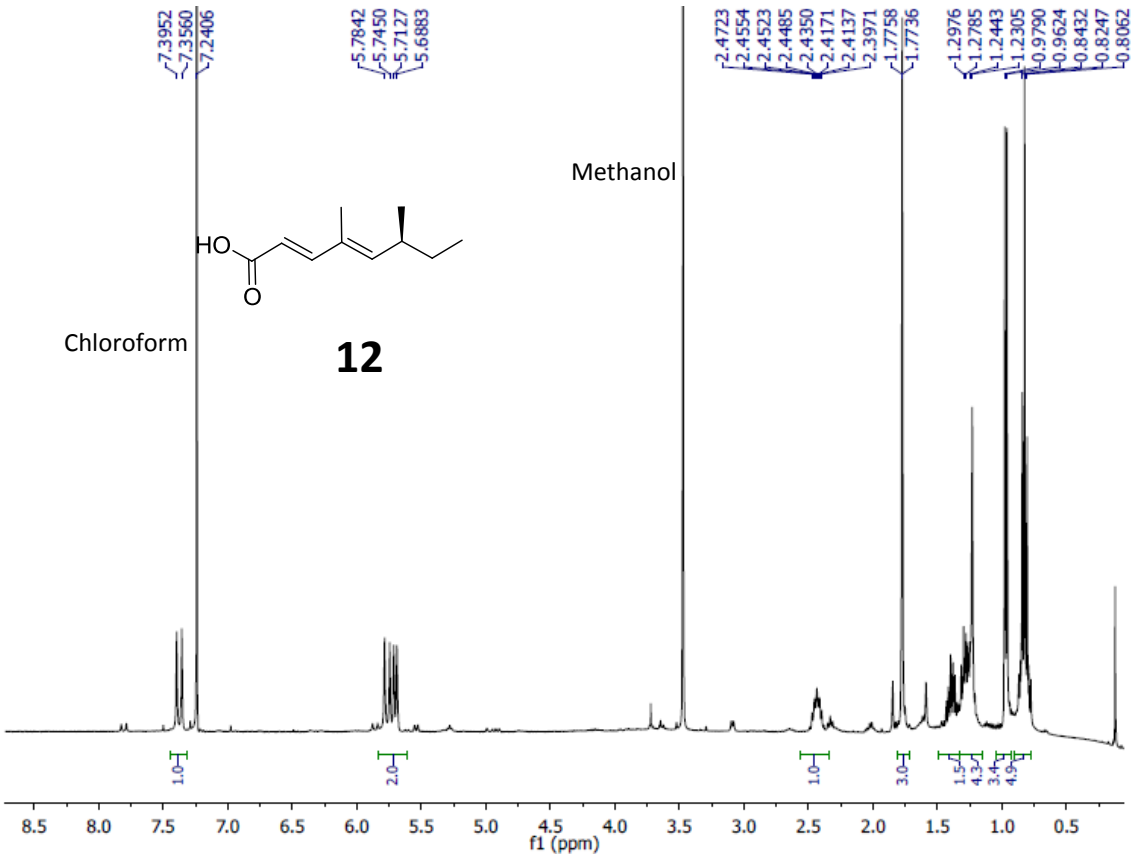

Figure S21. ^{1}H NMR Spectrum (400 MHz) of Compound 12 in $CDCl_3$.

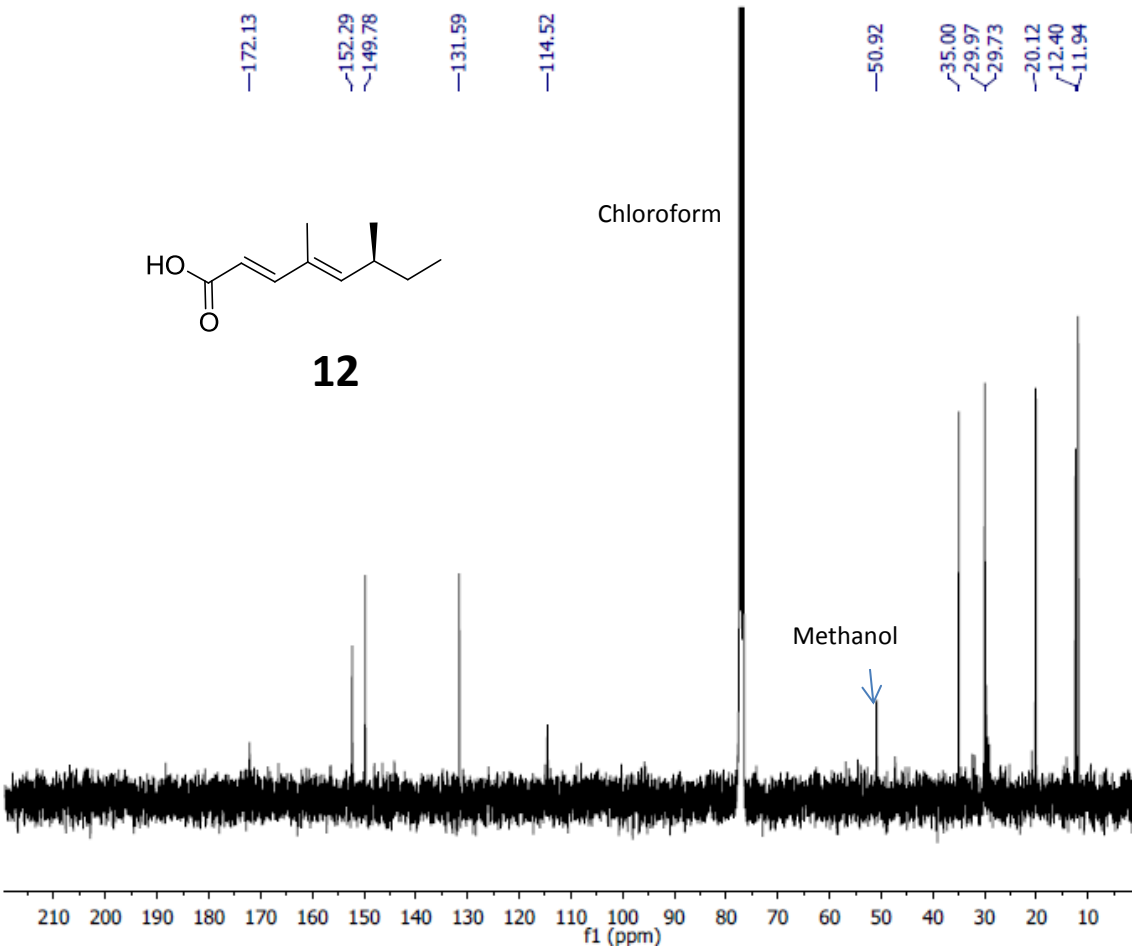

Figure S22. ^{13}C NMR Spectrum (100 MHz) of Compound 12 in $CDCl_3$

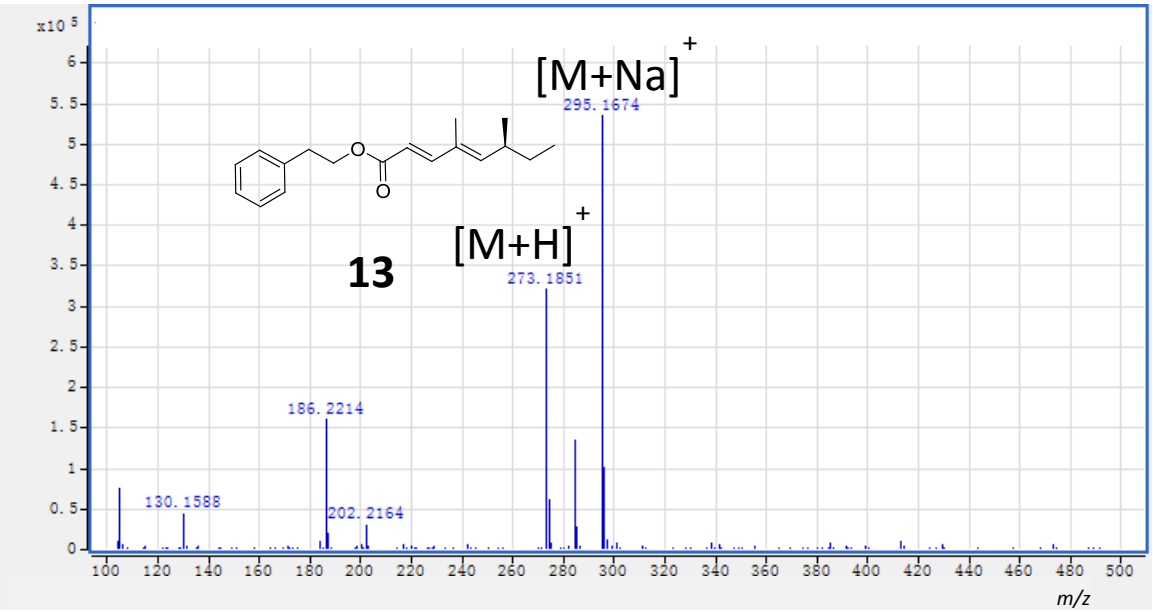

Figure S23. HR ESI-MS of Compound 13.

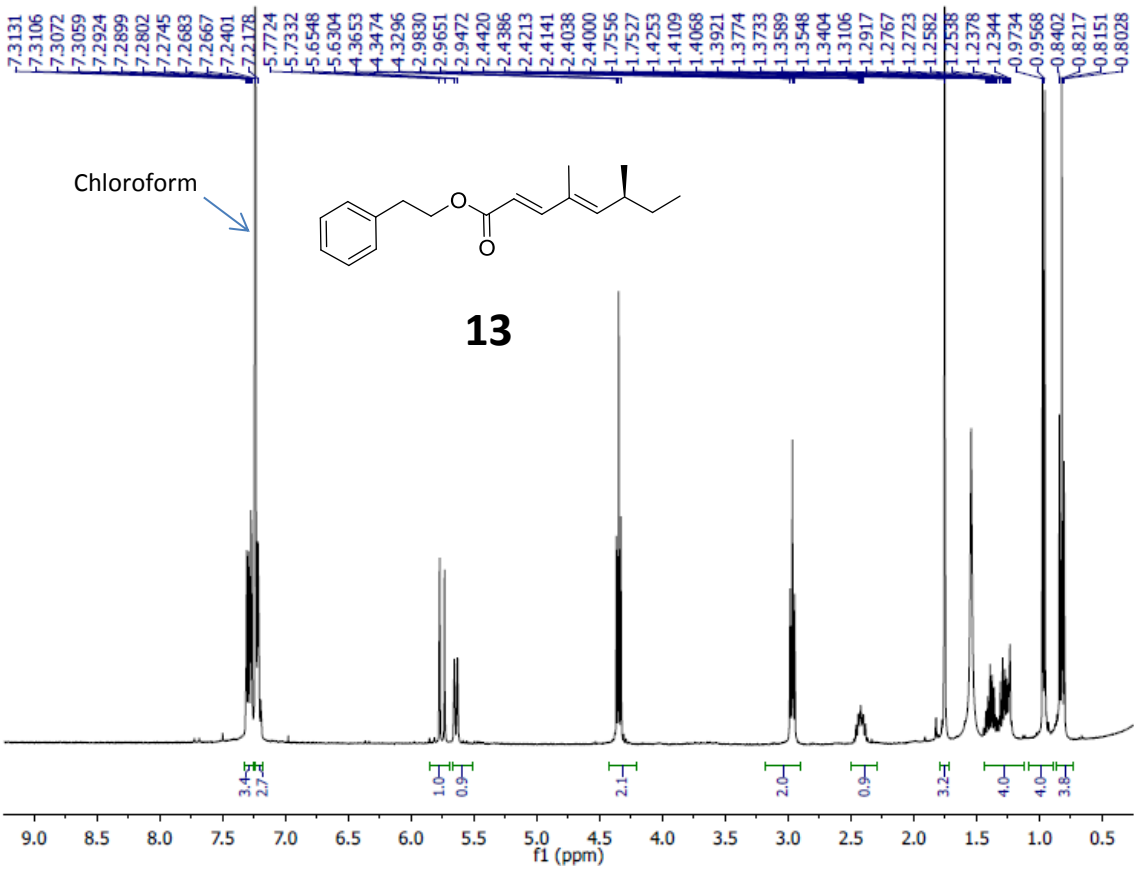

Figure S24. ^{1}H NMR Spectrum (400 MHz) of Compound 13 in $CDCl_3$.

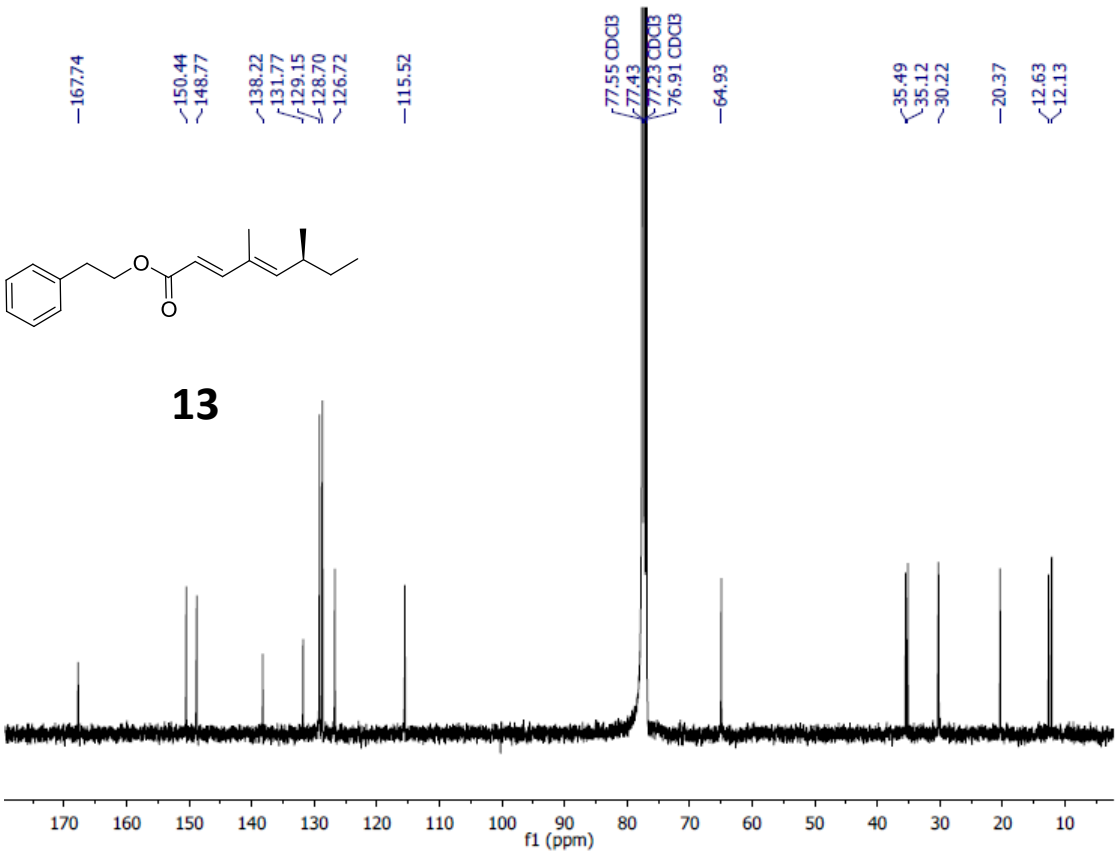

Figure S25. ^{13}C NMR Spectrum (100 MHz) of Compound 13 in $CDCl_3$.

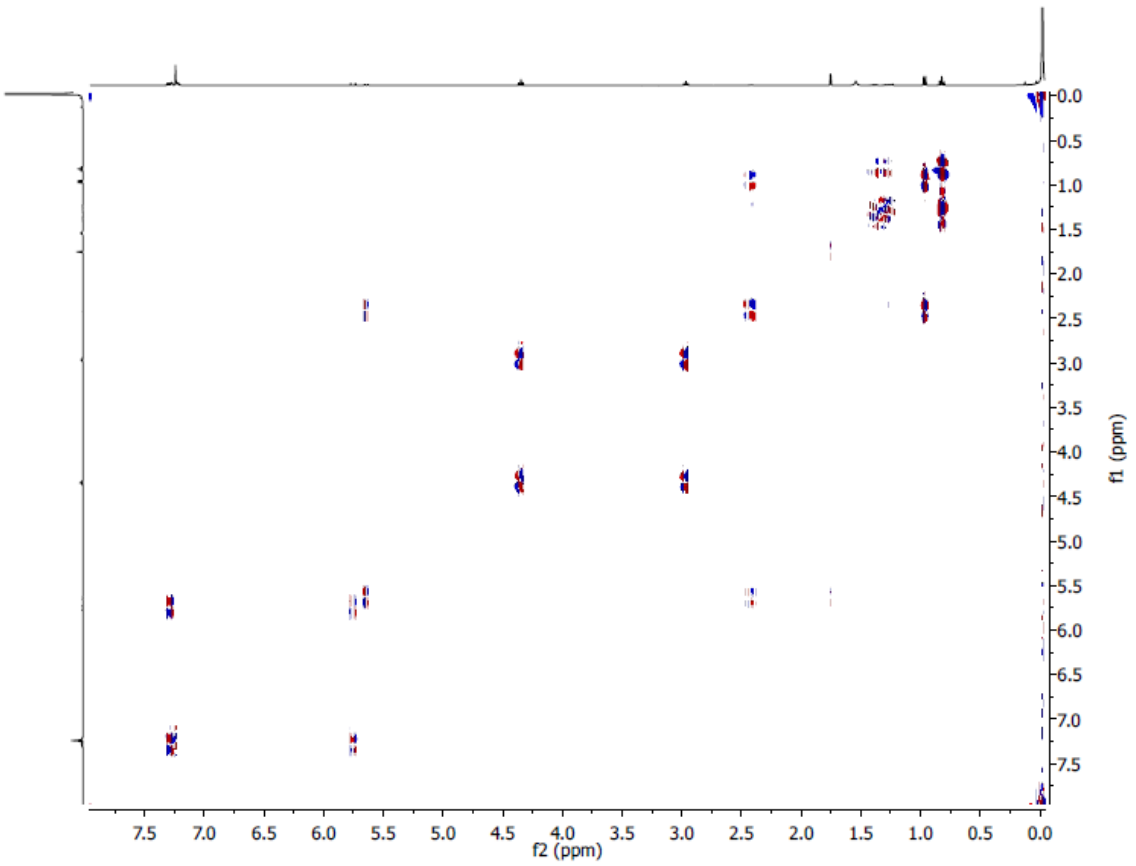

Figure S26. ^{1}H-^{1}H COSY Spectrum (400 MHz) of Compound 13 in $CDCl_3$.

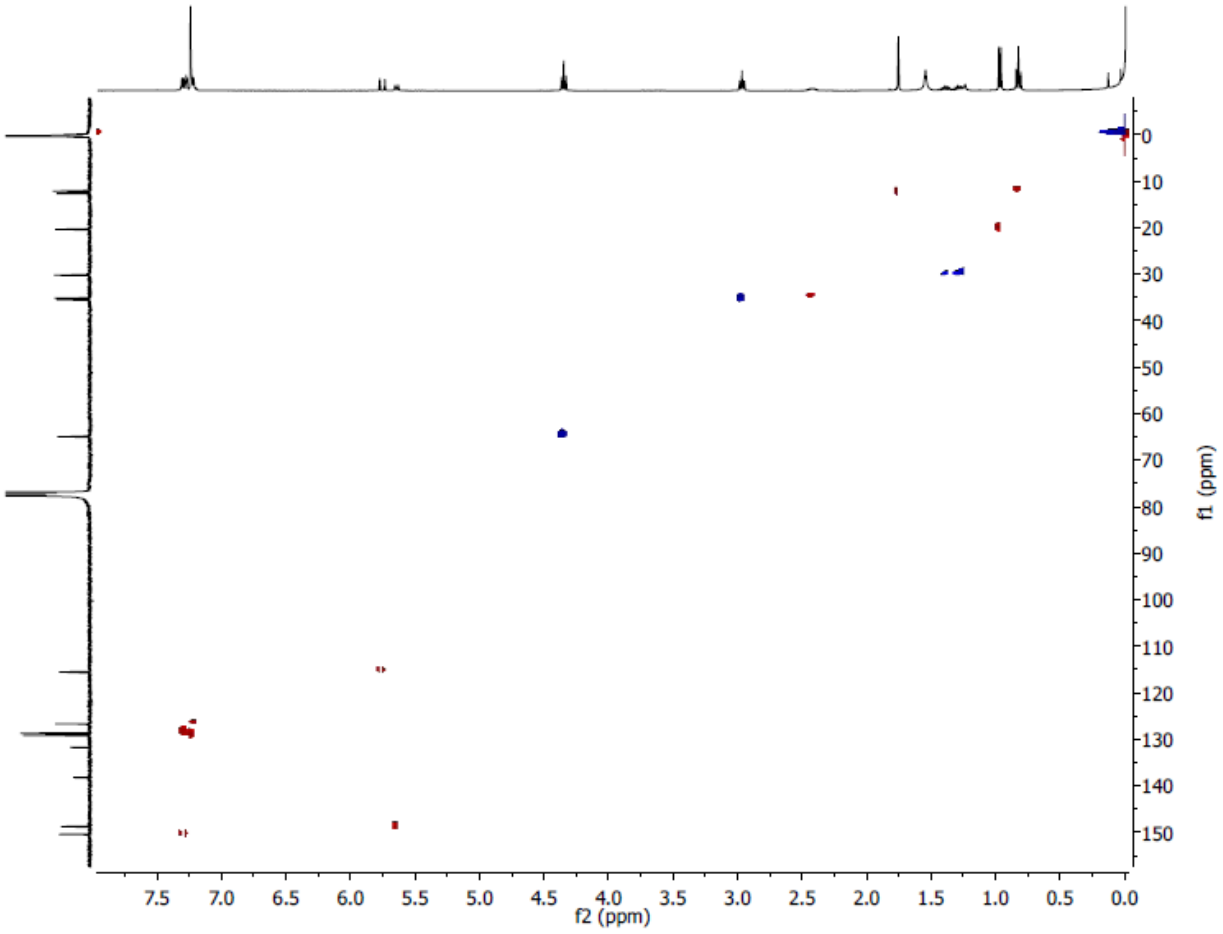

Figure S27. HSQC Spectrum (400 MHz) of Compound 13 in $CDCl_3$.

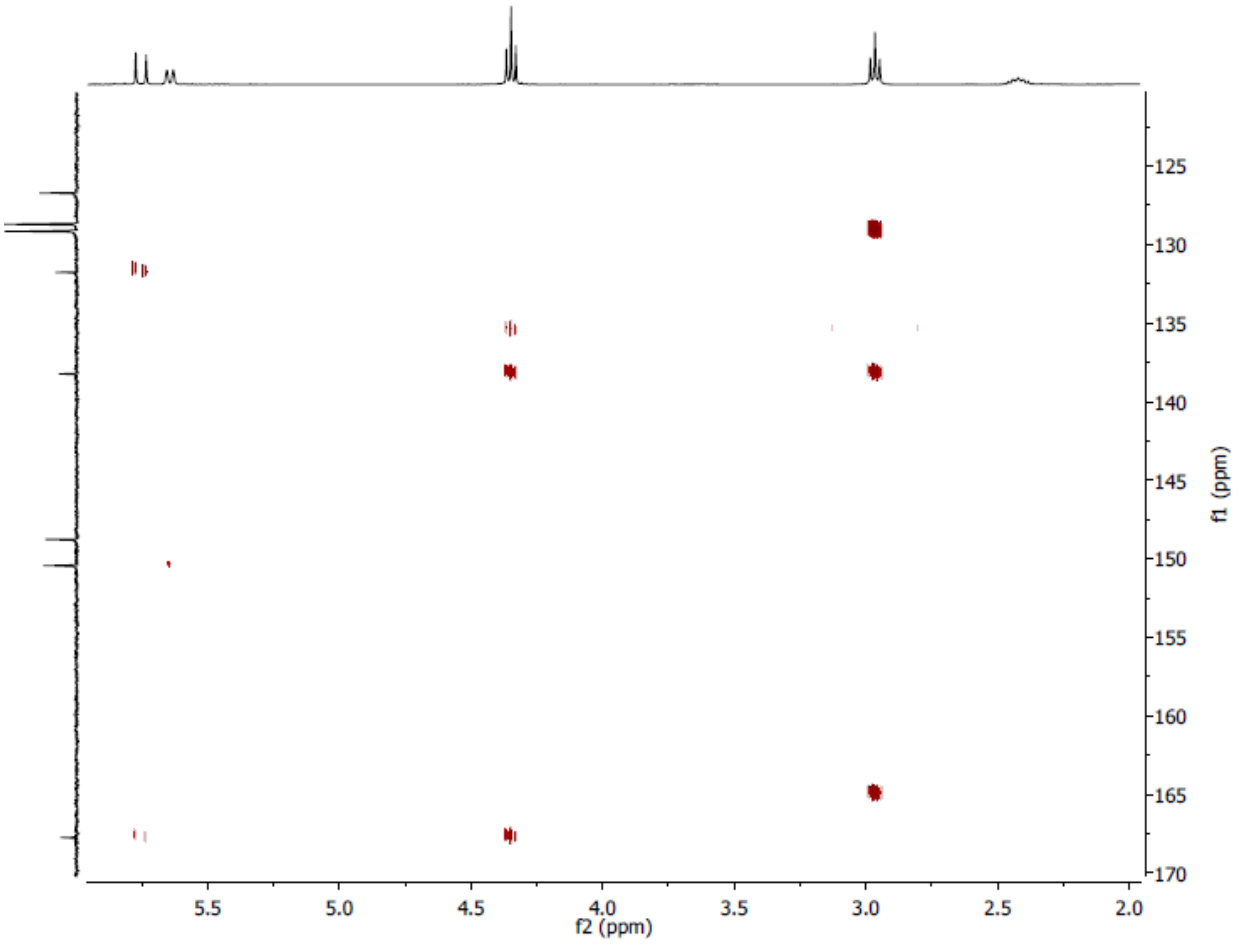

Figure S28. HMBC Spectrum (400 MHz) of Compound 13 in $CDCl_3$.

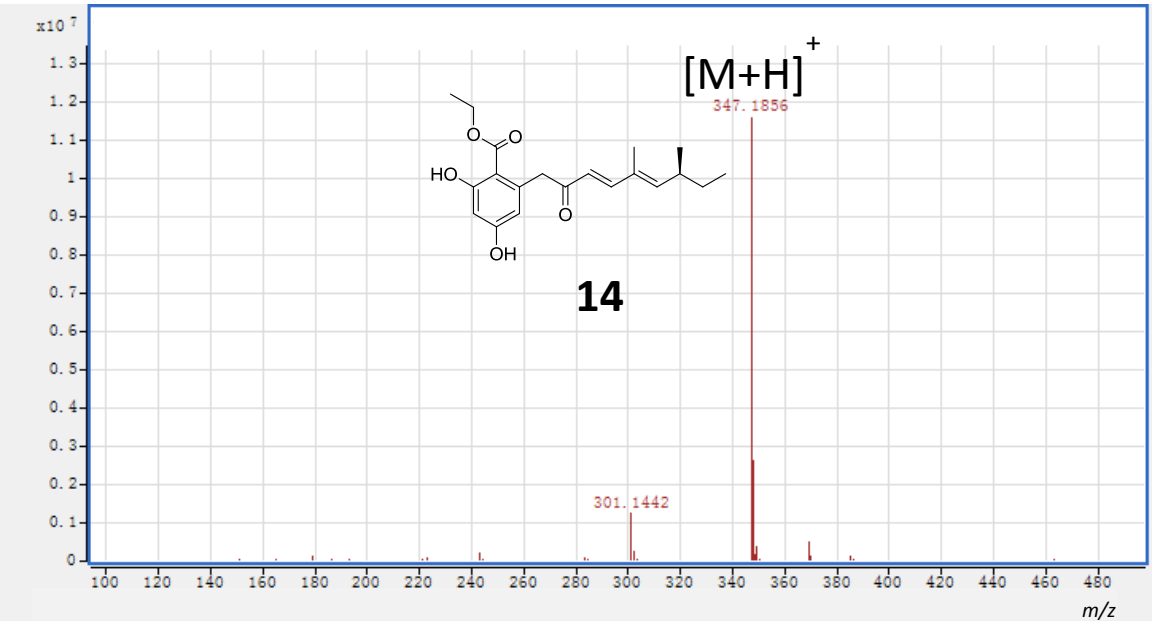

Figure S29. HR ESI-MS of Compound 14.

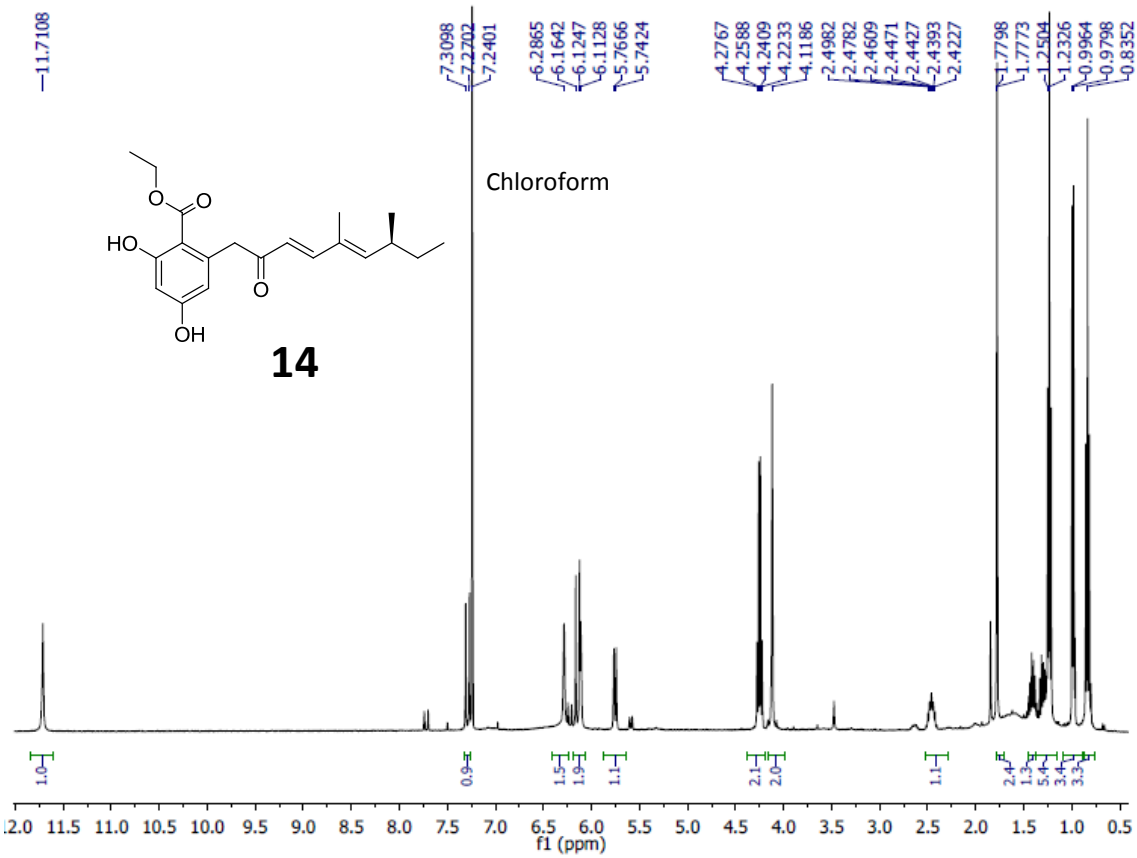

Figure S30. ^{1}H NMR Spectrum (400 MHz) of Compound 14 in $CDCl_3$.

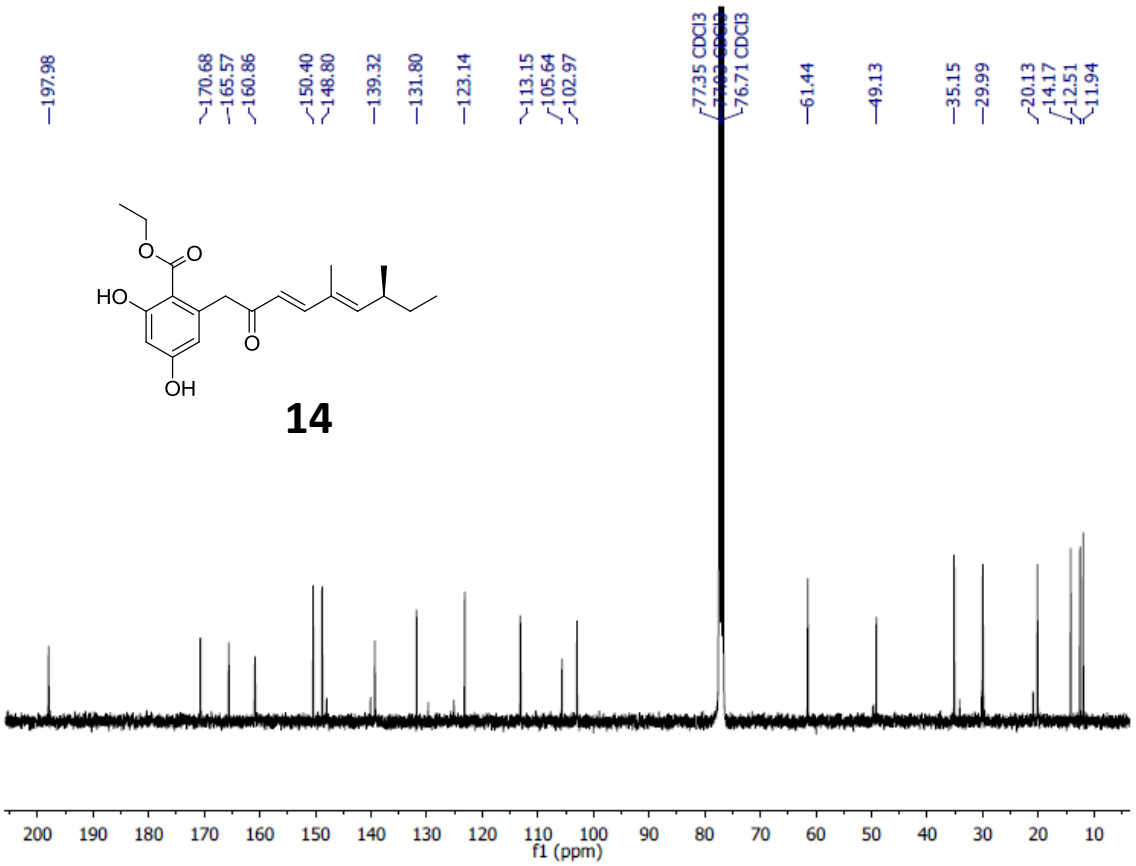

Figure S31. ^{13}C NMR Spectrum (400 MHz) of Compound 14 in $CDCl_3$.

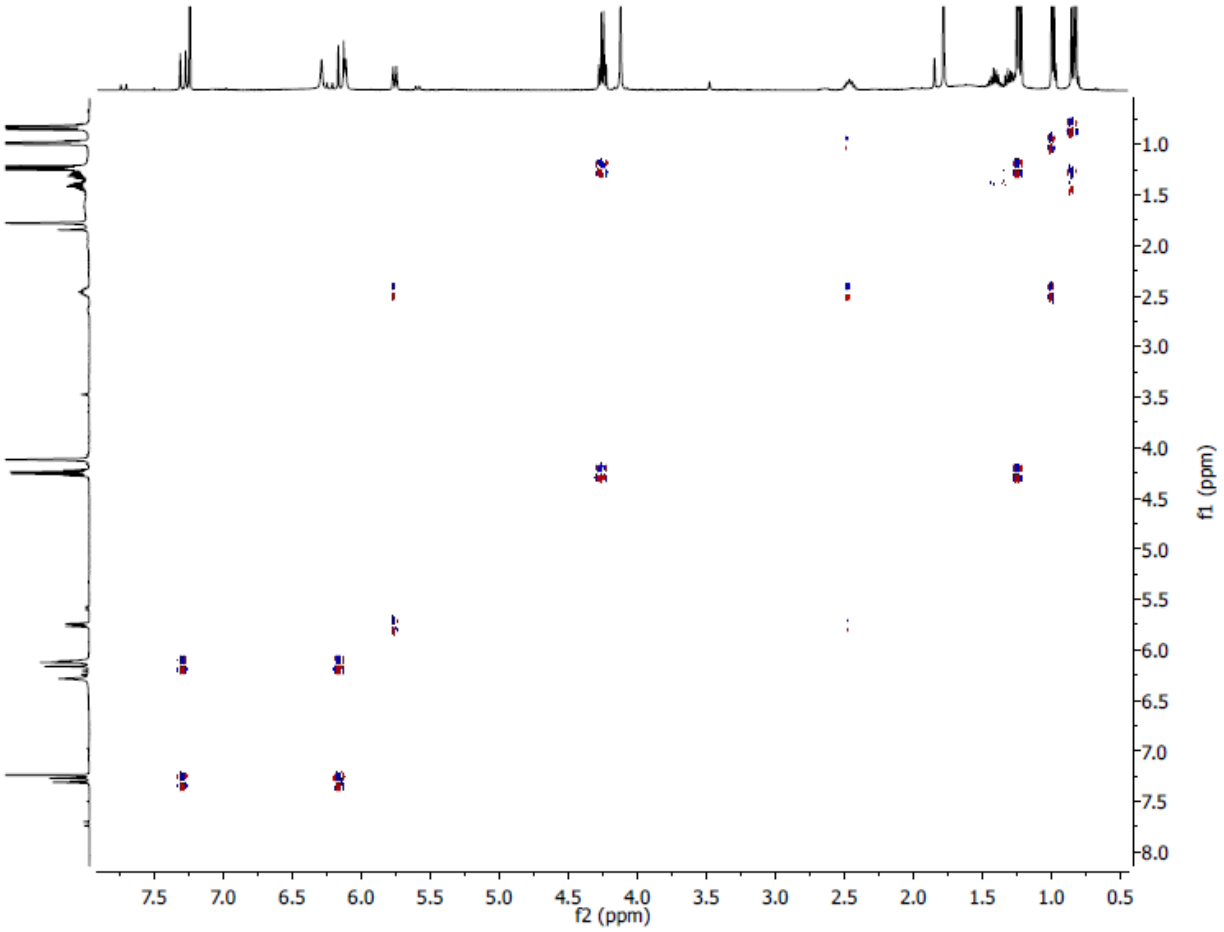

Figure S32. ^{1}H-^{1}H COSY Spectrum (400 MHz) of Compound 14 in $CDCl_3$.

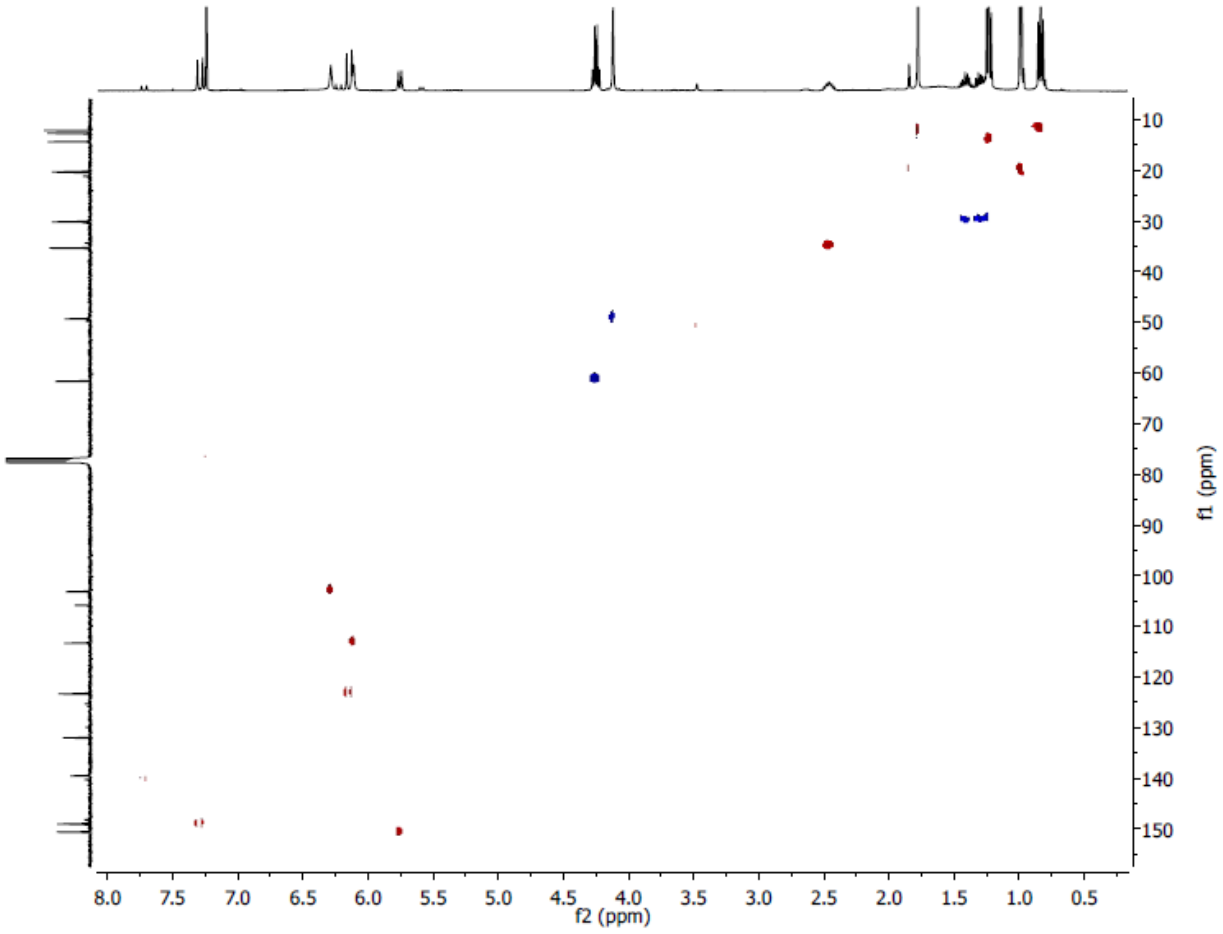

Figure S33. HSQC Spectrum (400 MHz) of Compound 14 in $CDCl_3$.

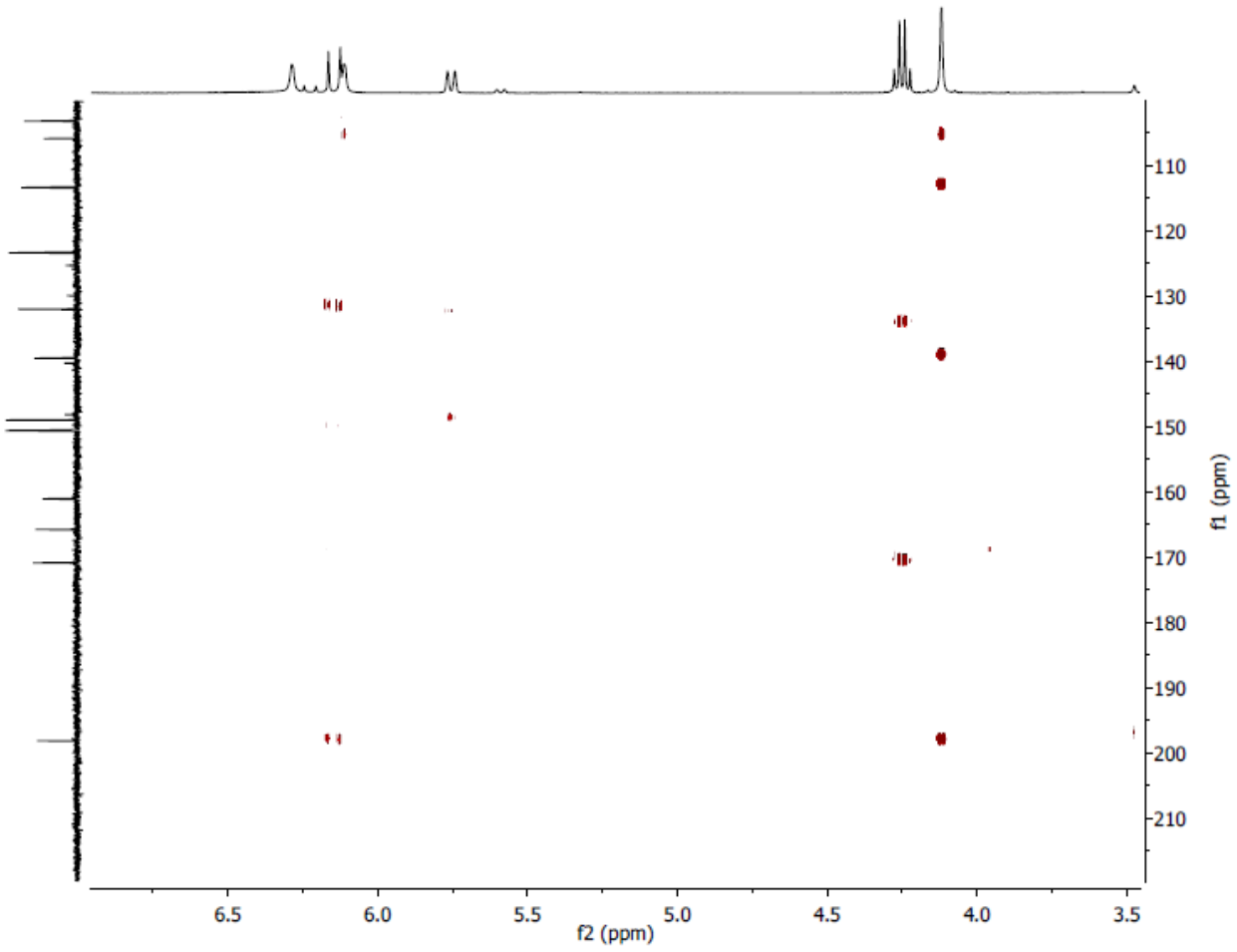

Figure S34. Key HMBC Spectrum (400 MHz) of Compound 14 in $CDCl_3$.

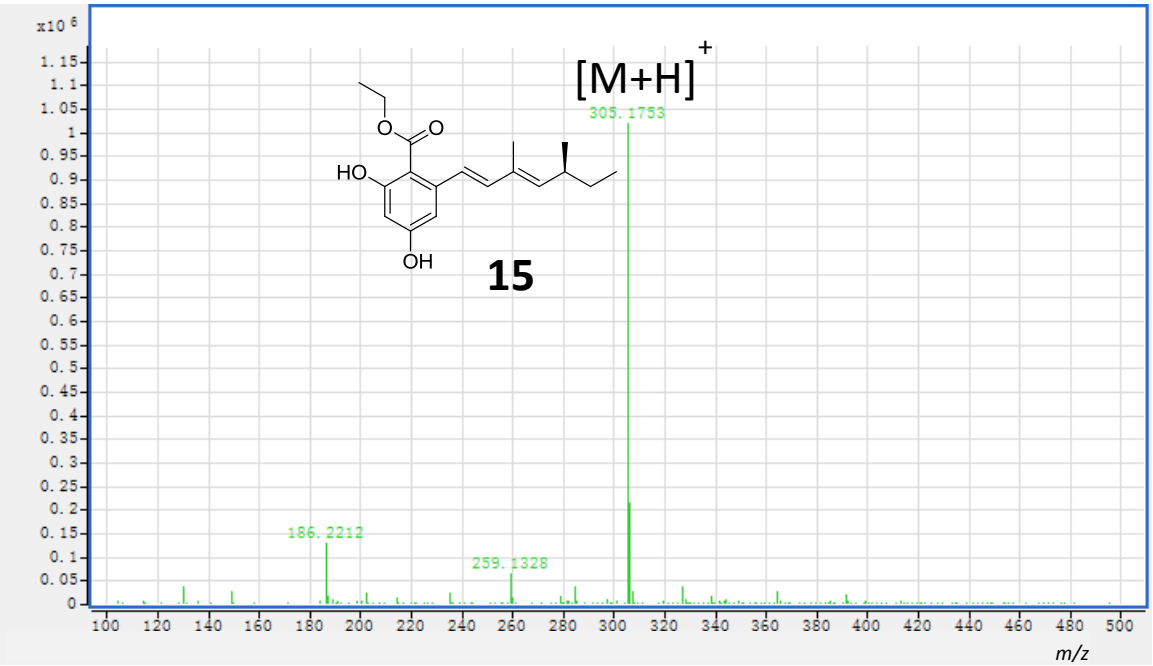

Figure S35. HR ESI-MS of Compound 15.

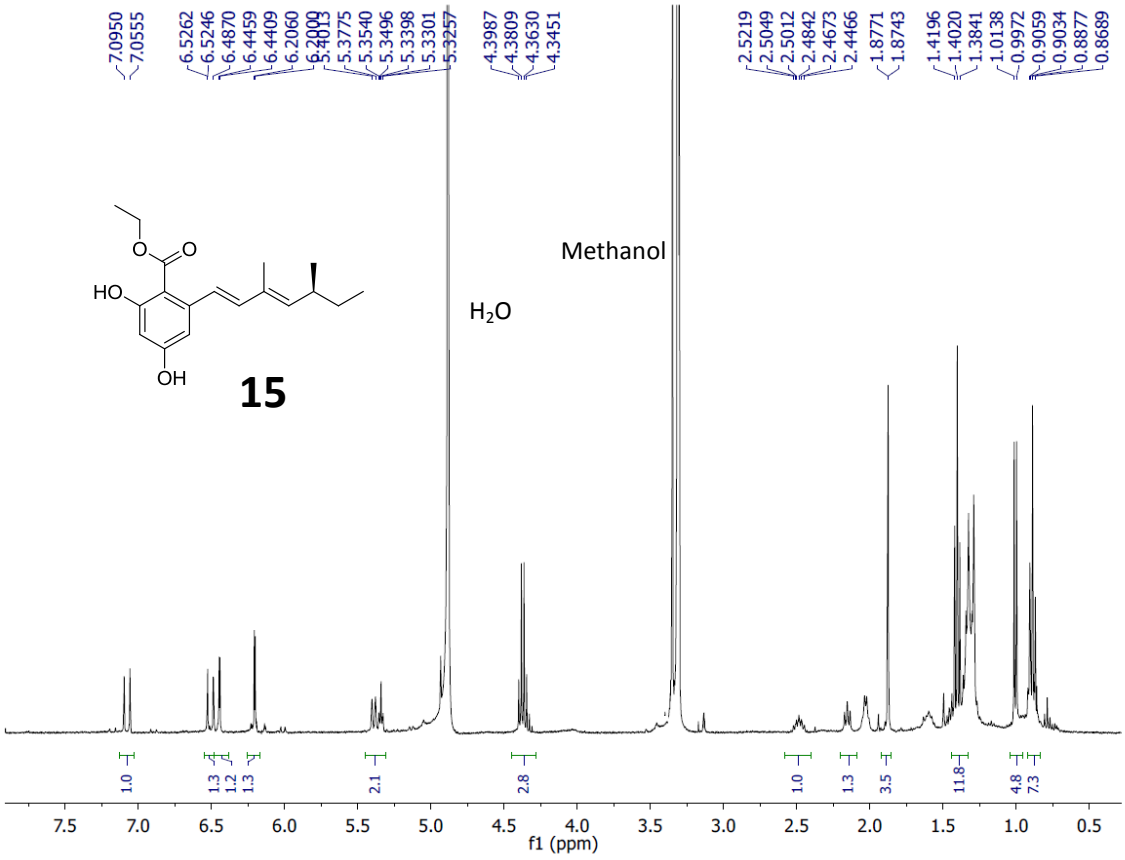

Figure S36. ^{1}H NMR Spectrum (400 MHz) of Compound 15 in CD_3OD.

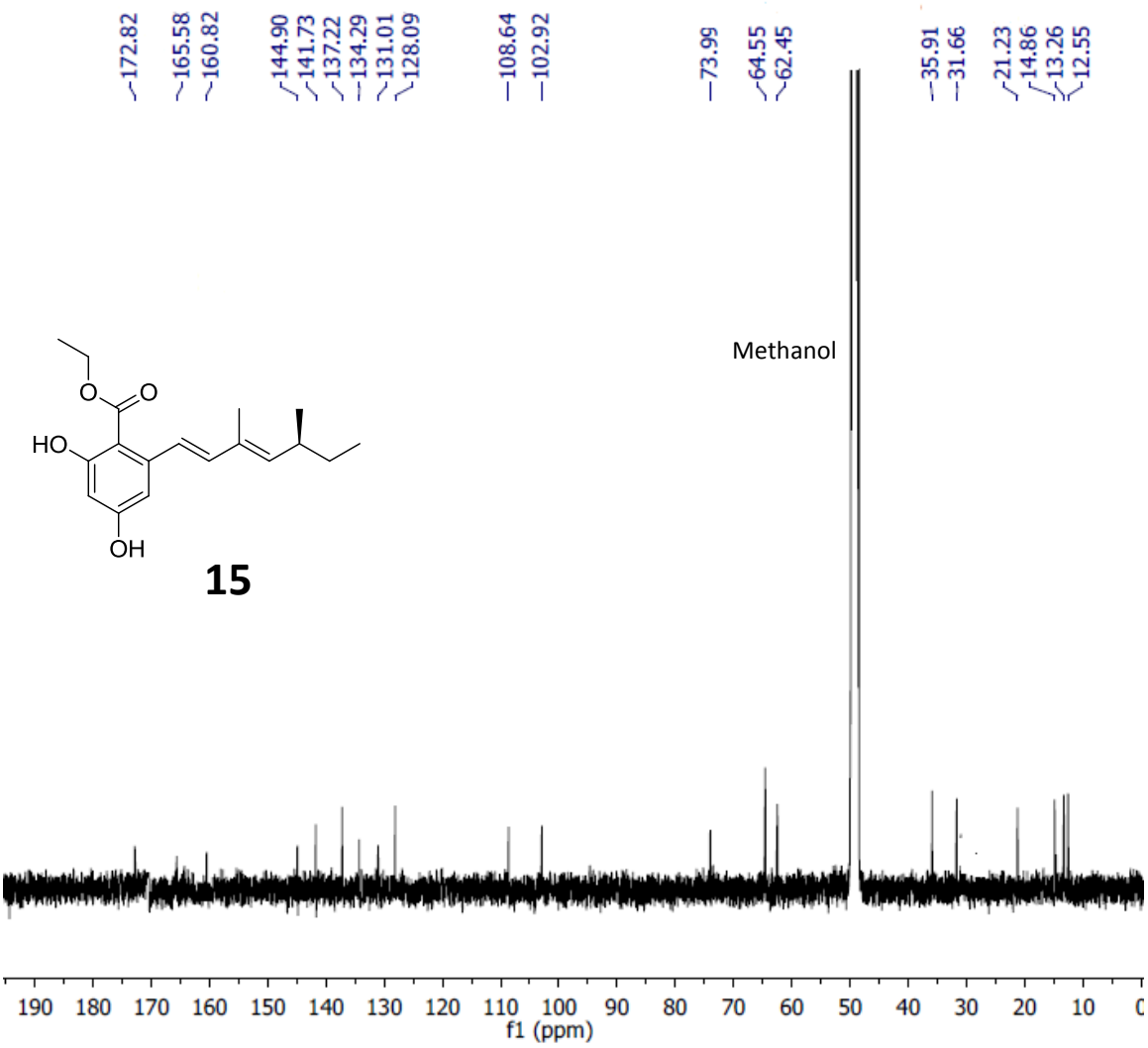

Figure S37. ^{13}C NMR Spectrum (100 MHz) of Compound 15 in CD_3OD.

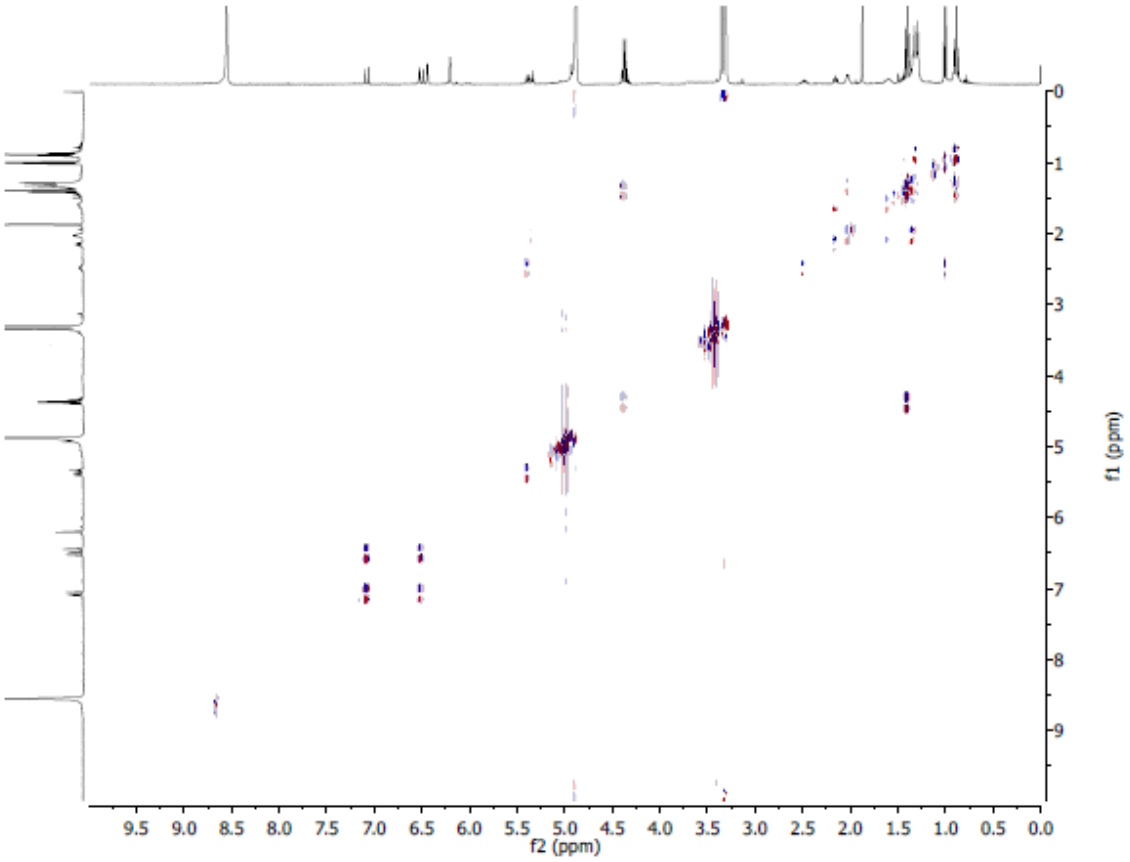

Figure S38. ^{1}H-^{1}H COSY Spectrum (400 MHz) of Compound 15 in CD_3OD.

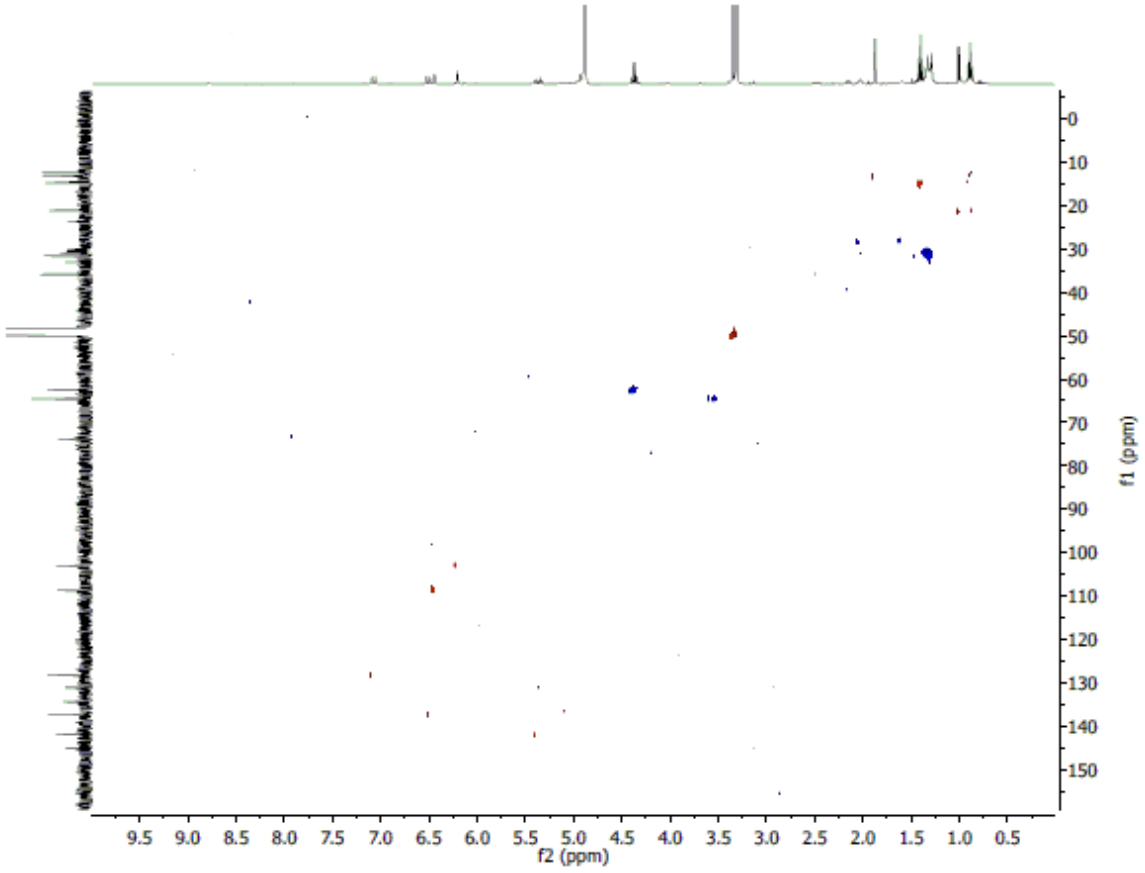

Figure S39. HSQC Spectrum (400 MHz) of Compound 15 in CD_3OD.

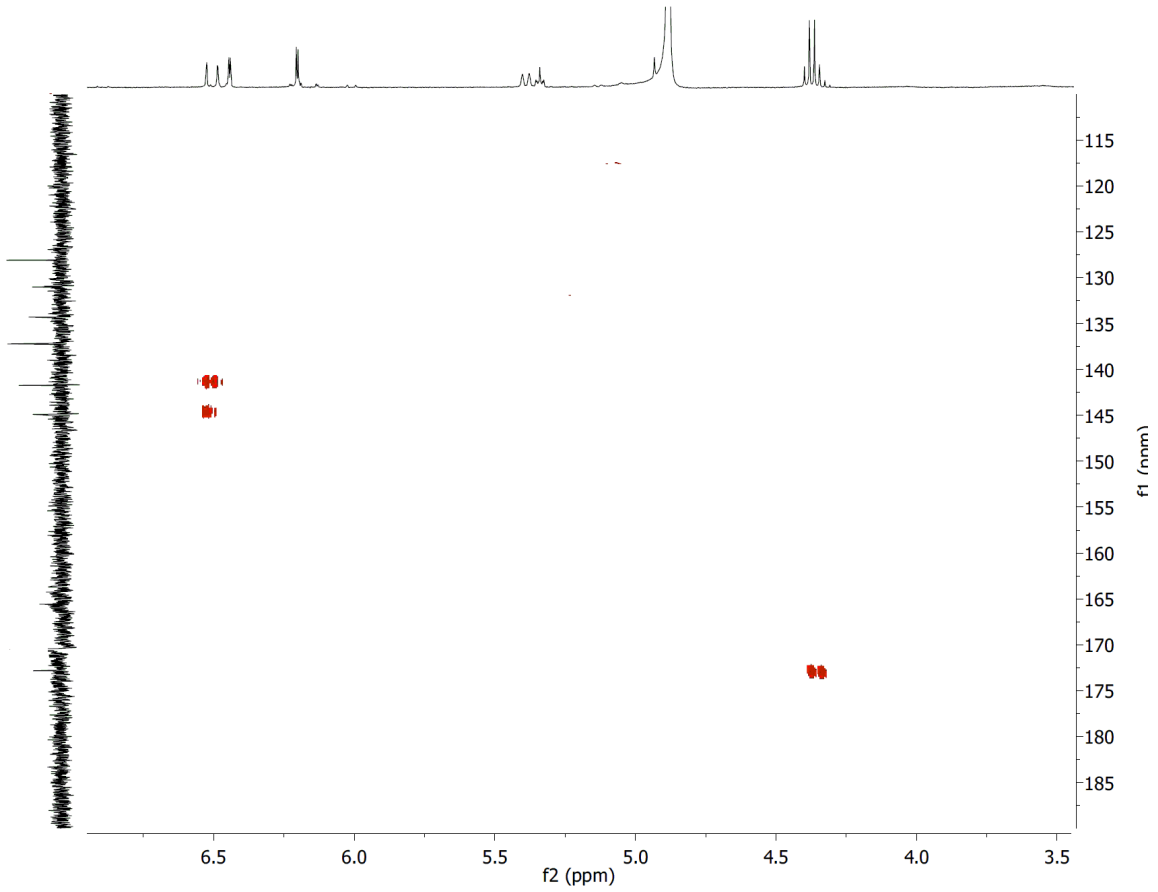

Figure S40. Key HMBC Spectrum (400 MHz) of Compound 15 in CD_3OD.

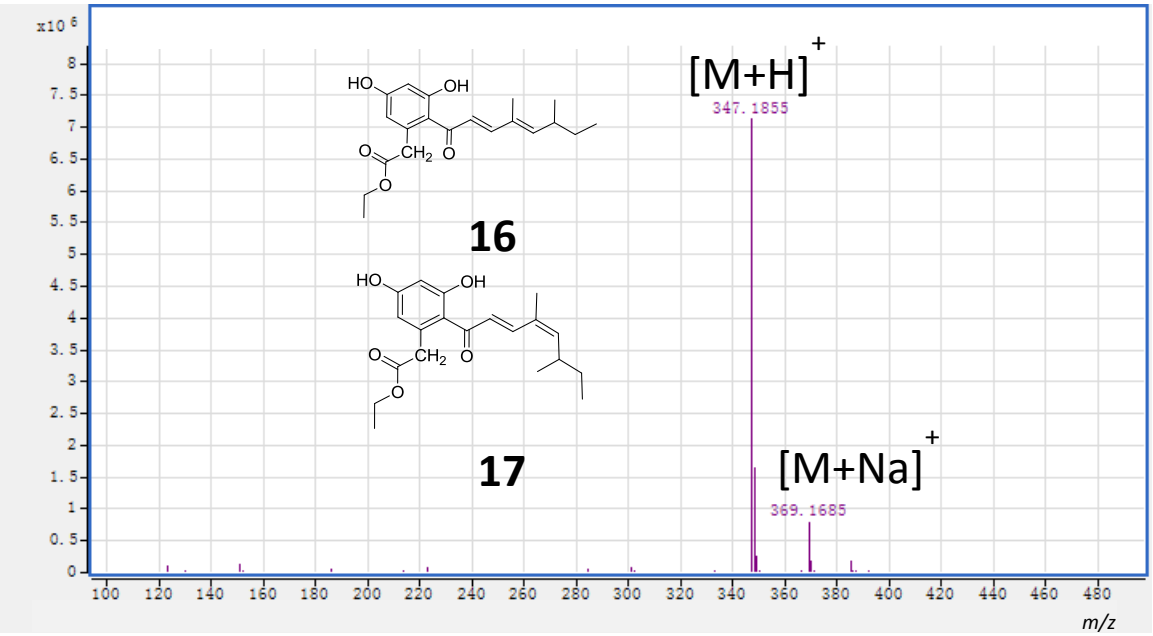

Figure S41. HR ESI-MS of Compounds 16/17.

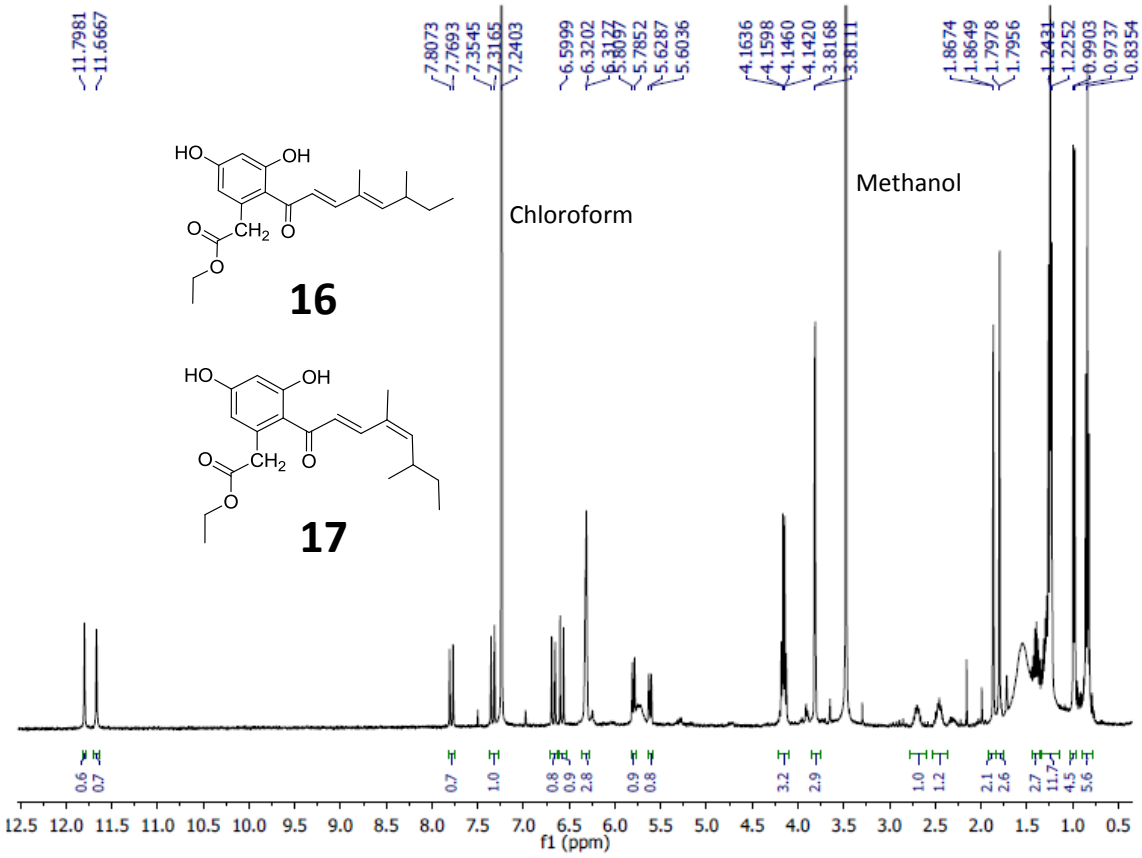

Figure S42. ^{1}H NMR Spectrum (400 MHz) of Compounds 16/17 in $CDCl_3$.

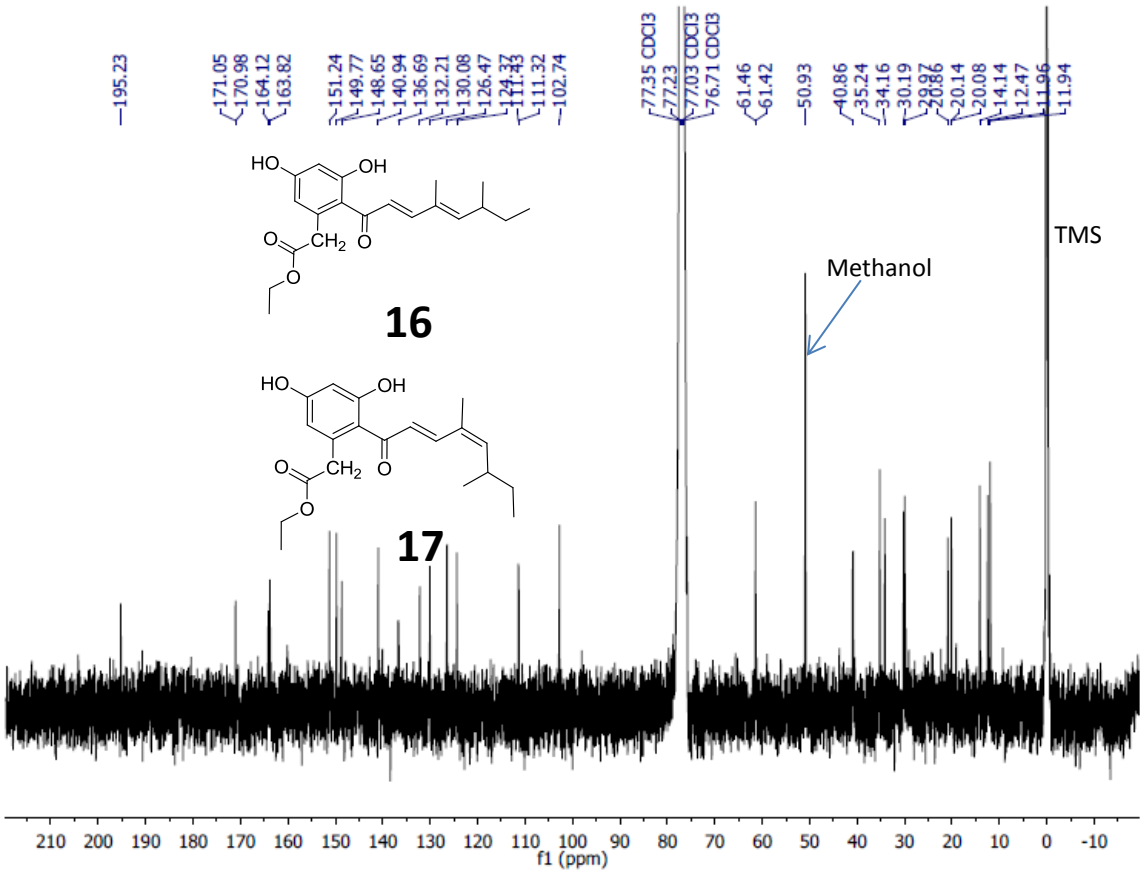

Figure S43. ^{13}C NMR Spectrum (100 MHz) of Compounds 16/17 in $CDCl_3$.

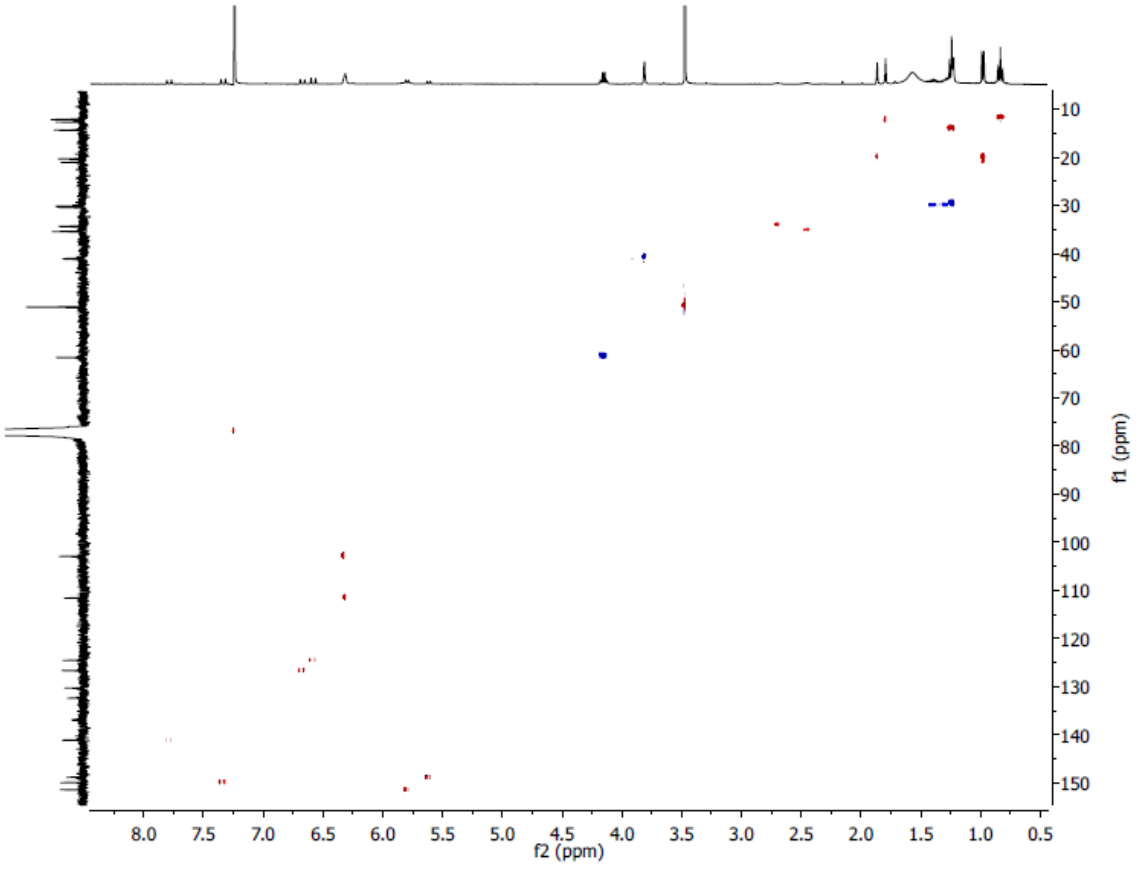

Figure S44. HSQC Spectrum (400 MHz) of Compounds 16/17 in $CDCl_3$.

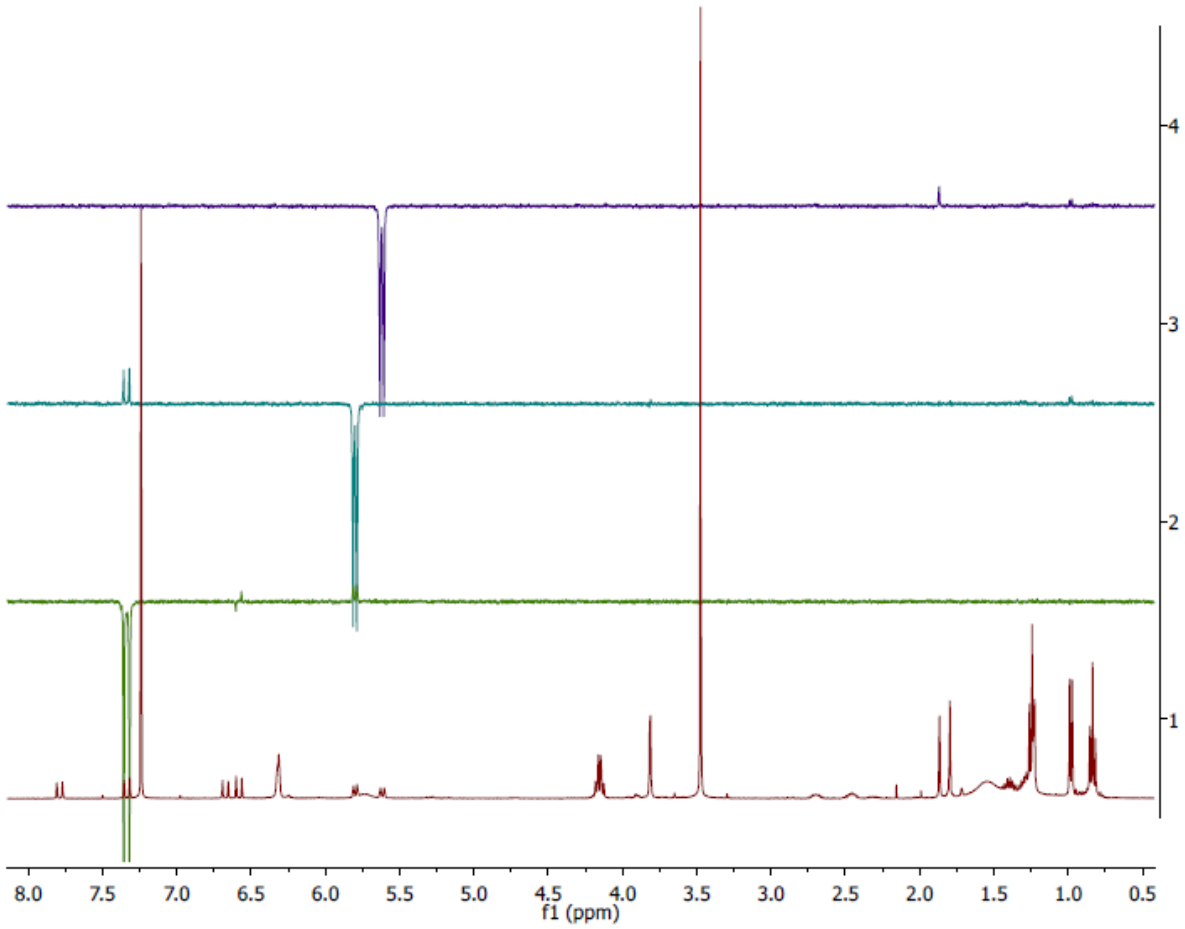

Figure S45. 1D NOESY Spectra (400 MHz) of Compounds 16/17 in $CDCl_3$.

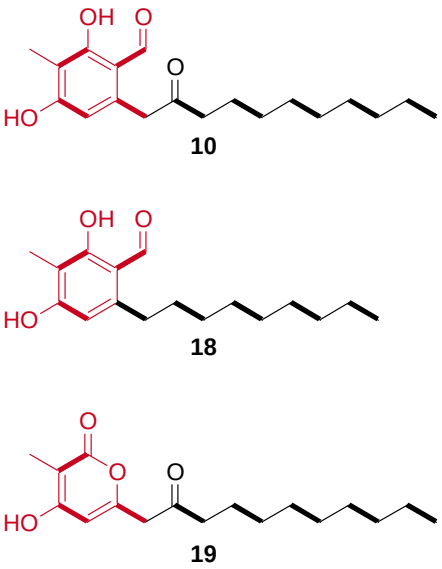

Figure S46. Comparison of the chemical structures of compounds 10, 18[15] and 19[15]

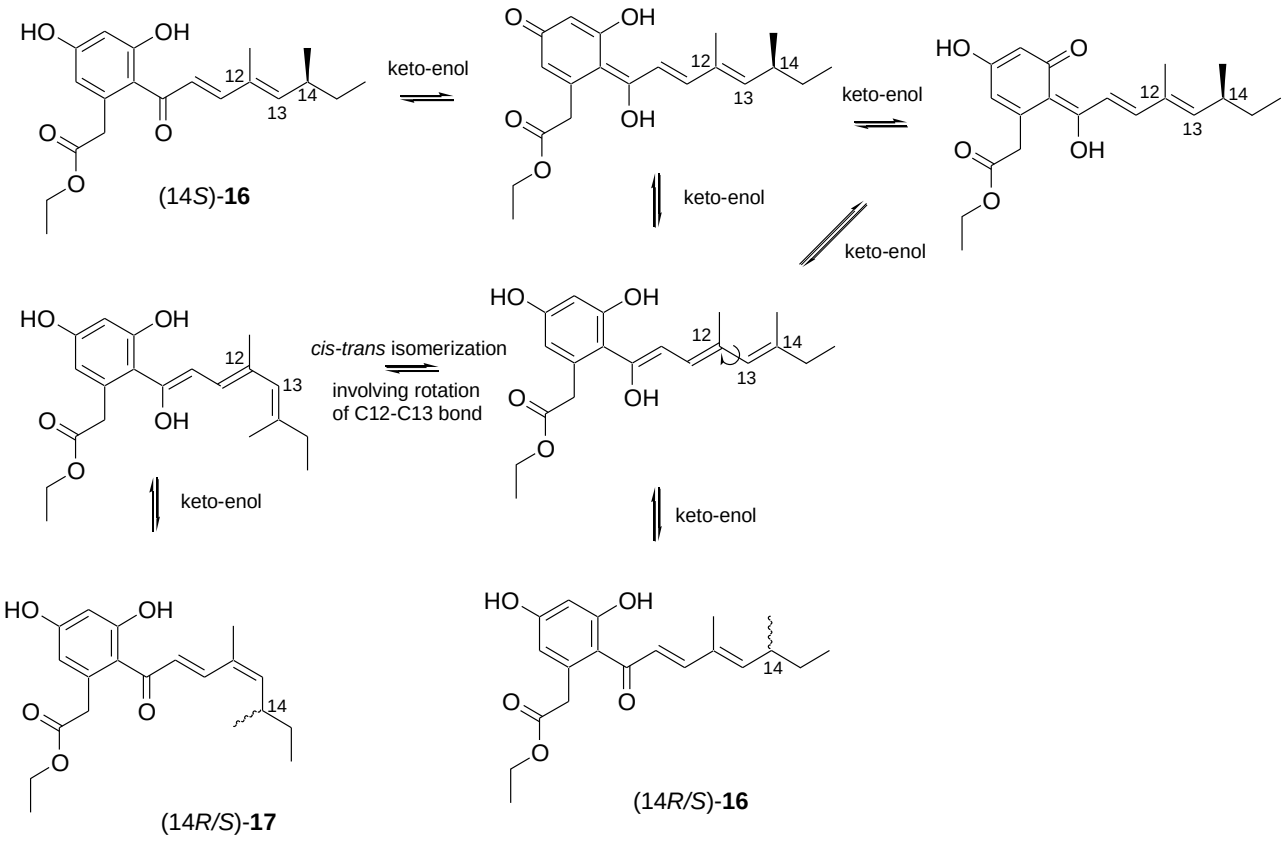

Figure S47. Proposed mechanism for *E/Z* isomerization with concomitant racemization to form 16 and 17.

The *E/Z* isomerization at C12(13) with concomitant racemization at C14 of natural (14*S*)-**16** is proposed to involve a plausible keto-enol-type tautomerization and *cis-trans* isomerization during fermentations and/or workup of the resulting extracts to yield an inseparable mixture of (14*R*/*S*)-**16** and (14*R/S*)-**17**.

5. SI References

(1) Xu, Y.; Zhou, T.; Espinosa-Artiles, P.; Tang, Y.; Zhan, J.; Molnár, I. *ACS Chem. Biol.* **2014**, *9*, 1119.

(2) Xu, Y.; Zhou, T.; Zhang, S.; Xuan, L. J.; Zhan, J.; Molnár, I. *J. Am. Chem. Soc.* **2013**, *135*, 10783.

(3) Xu, Y.; Zhou, T.; Zhou, Z.; Su, S.; Roberts, S. A.; Montfort, W. R.; Zeng, J.; Chen, M.; Zhang, W.; Zhan, J.; Molnár, I. *Proc. Natl. Acad. Sci. U.S.A.* **2013**, *110*, 5398.

(4) Xu, Y.; Espinosa-Artiles, P.; Schubert, V.; Xu, Y. M.; Zhang, W.; Lin, M.; Gunatilaka, A. A. L.; Süssmuth, R.; Molnár, I. *Appl. Environ. Microbiol.* **2013**, *79*, 2038.

(5) Udwary, D. W.; Merski, M.; Townsend, C. A. *J. Mol. Biol.* **2002**, *323*, 585.

(6) Christianson, T. W.; Sikorski, R. S.; Dante, M.; Shero, J. H.; Hieter, P. *Gene* **1992**, *110*, 119.

(7) Zhou, H.; Qiao, K.; Gao, Z.; Vederas, J. C.; Tang, Y. *J. Biol. Chem.* **2010**, *285*, 41412.

(8) Ma, S. M.; Li, J. W.; Choi, J. W.; Zhou, H.; Lee, K. K.; Moorthie, V. A.; Xie, X.; Kealey, J. T.; Da Silva, N. A.; Vederas, J. C.; Tang, Y. *Science* **2009**, *326*, 589.

(9) Chiang, Y. M.; Szewczyk, E.; Davidson, A. D.; Keller, N.; Oakley, B. R.; Wang, C. C. *J. Am. Chem. Soc.* **2009**, *131*, 2965.

(10) Jones, G. B.; Huber, R. S.; Chapman, B. J. *Tetrahedron: Asym.* **1997**, *8*, 1797.

(11)Ahuja, M.; Chiang, Y. M.; Chang, S. L.; Praseuth, M. B.; Entwistle, R.; Sanchez, J. F.; Lo, H. C.; Yeh, H. H.; Oakley, B. R.; Wang, C. C. *J. Am. Chem. Soc.* **2012**, *134*, 8212.

(12) Yoshida, E.; Fujimoto, H.; Baba, M.; Yamazaki, M. *Chem. Pharm. Bull.* **1995**, *43*, 1307.

(13) Zhu, J.; Grigoriadis, N. P.; Lee, J. P.; Porco, J. A. *J. Am. Chem. Soc.* **2005**, *127*, 9342.

(14) Matsuzaki, K.; Tahara, H.; Inokoshi, J.; Tanaka, H.; Masuma, R.; Omura, S. *J. Antibiot.* **1998**, *51*, 1004.

(15) Liu, T.; Sanchez, J. F.; Chiang, Y. M.; Oakley, B. R.; Wang, C. C. *Org. Lett.* **2014**, *16*, 1676.

(16) Liu, T.; Chiang, Y. M.; Somoza, A. D.; Oakley, B. R.; Wang, C. C. *J. Am. Chem. Soc.* **2011**, *133*, 13314.